The usefulness of Total Runoff Integrating Pathways (TRIP) for validating land surface models

Master's Thesis
Meteorology, Physical Oceanography and Climate
Utrecht University and Royal Dutch Meteorological Institute (KNMI)

Cynthia Maan

December 2009

Supervisors:
Prof. dr. B.J.J.M. van den Hurk
Dr. F. Pappenberger

Summary

In this study, the usefulness of the global river routing model Total Runoff Integrating Pathways (TRIP) for the validation of land surface models is discussed. An attempt is made to compare and validate the modeled runoff of two different land modules of the climate model EC-EARTH: the Tiled ECMWF Surface Scheme for Exchange over Land (TESSEL) and the revised Hydrology Tiled ECMWF Surface Scheme for Exchange over Land (HTESSEL). These land surface models especially differ in the generation of surface runoff, which results in high frequency variability in the modeled runoff. To validate the TESSEL and HTESSEL models in terms of runoff, the modeled river discharge of the Danube and the Amazon rivers are compared with observations.

It is concluded that the usefulness of the TRIP scheme for the validation of the land surface models is limited by its tendency to delay the water too much and to filter out high frequency variability. For comparison, a simple method was used to estimate the river discharges without river routing. For this approach, the unrouted runoff was manipulated by applying a time shift and smoothing the data over a certain time period. The method was applied for a couple of rivers. The quality of the obtained results are at least comparable with the TRIP simulations. This might suggest that the TRIP scheme is unnecessary complicated for its purpose.

By comparing the high frequency variability in the unrouted runoff directly with the discharge observations it is found that the TESSEL scheme underestimates the high frequency variability in the runoff in the Danube region. Estimates of the river discharge that were found by a simple manipulation on the HTESSEL runoff suggest that the high frequency variability in the runoff is well modeled by the HTESSEL scheme in the Danube region. In the Amazon, both offline models perform equally bad and underestimate the runoff by about 60% (due to too much evaporation). A large underestimation of the runoff was also found in the Mississippi region.

An attempt has also been made to compare the behavior of the TESSEL and HTESSEL land modules in an online model simulation, where the LSMs were coupled to the climate model EC-EARTH. Online validation seems to be difficult due to uncertainties in the climate model. The climate simulation of the surface water balance is especially influenced by the modeled precipitation that drives the land surface scheme. Due to errors in the modeled precipitation it is difficult to compare the offline and online behavior of the land surface models. In most areas that were considered, the precipitation was (in various extents) underestimated by the climate model. A comparison between the online and offline modeled runoff indicates that in most areas the underestimation of the precipitation by the climate model leads to a reduction in the modeled evaporation (rather than to a reduction in the runoff). In the Danube region, the correlation between the runoff and the precipitation is under-represented by the climate model. These features indicate that the atmospheric conditions in the climate model might be different from the observed atmospheric conditions. It is not clear whether this difference should be ascribed to the effect of the land surface model on the atmosphere or to errors in the atmospheric model itself.

Contents

1

Introduction

1.1 Land surface and climate

Already for a long time now, people recognize the influence that the land surface has on earth's climate. For instance, the biography of Christopher Columbus, written by his son, states:

> "On Tuesday, July 22nd [1494] , he departed for Jamaica.... The sky, air and climate were just the same as in other places; every afternoon there was a rain squall that lasted for about an hour. The admiral writes that he attributes this to the great forests of the land; he knew from experience that formerly this also occurred in the Canary, Madeira, and Azore Islands, but since the removal of forests that once covered those islands they do not have so much mist and rain as before."

Earh's climate is influenced by the land surface in many ways. For instance, mountain chains such as the Andes or the Rocky Mountains are influencing the climate by forming barriers to the westerly winds and by affecting planetary waves and the global atmospheric circulation. The presence of land boundaries to the ocean affects the location of the strong western boundary currents (Goosse et al, 2009) [5].

The land surface also plays a more active role in weather and climate. It does so mainly by soil and vegetation processes that exchange carbon (figure 1.1), water and energy with

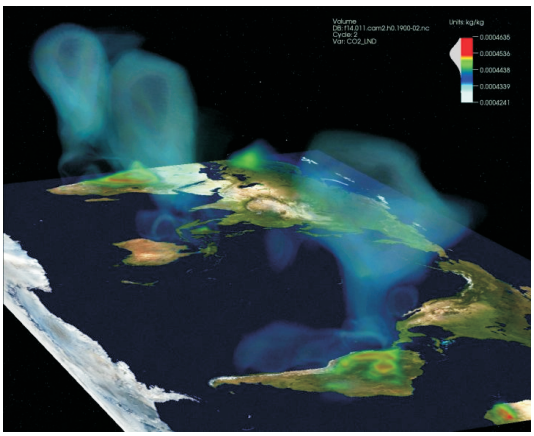

Figure 1.1: *Atmospheric carbon dioxide originating from various sources on the land surface in February 1990. The carbon concentration is illustrated as light colored plumes, ranging from 0.00004241(white/light blue) to 0.0004635 (red) kg CO_2 per kg of air. Exchange of carbon dioxide between land surface and atmosphere is especially large in vegetated areas as the Amazon. This visualization is made by Jamison Daniel and Forrest Hoffman of National Center for Computational Science and Oak Ridge National Laboratory.*

the atmosphere. For instance, vegetation cover has a large impact on the hydrological cycle. If precipitation (rain or snow) falls on the land surface, it is partitioned into evapotranspiration (the sum of evaporation and plant transpiration), infiltration (water that infiltrates into the soil) and surface runoff (water that runs off at the surface, following rivers towards the ocean). The exact partition between these components depends heavily on the ground and vegetation type. Water storage is generally greater in soil covered by vegetation than on rocks where most precipitation runs off at the surface. Stored water can later be taken up by plant roots and transferred back to the atmosphere by evapotranspiration or it runs off as deep-drainage (which, after some delay, enters the river streams to flow towards the ocean). Evapotranspiration from the vegetation and soil-interface influences the atmosphere at short time scales, whereas the storage of water in the soil influences the low frequency atmospheric variability.

Land surface processes are not only influencing climate, but in turn, climate is also influencing the land surface. The type and the presence of vegetation depends on temperature and precipitation. If temperature or precipitation is too low, desert will dominate. The interaction between land surface and climate leads to powerful feedbacks. Therefore, an important component in understanding climate change is understanding the processes that determine the exchange of carbon, water and energy between land surface and atmosphere.

1.2 Modeling land surface processes

To perform climate simulations and predictions and weather forecasting, mathematical models have been constructed that describe the physical processes in the atmosphere, ocean and land surface. These Global Climate Models (GCMs) consist of Atmospheric and Oceanic General Circulation Models (AGCMs and OGCMs) along with sea-ice and land-surface models (SIMs and LSMs; see figure 1.2).

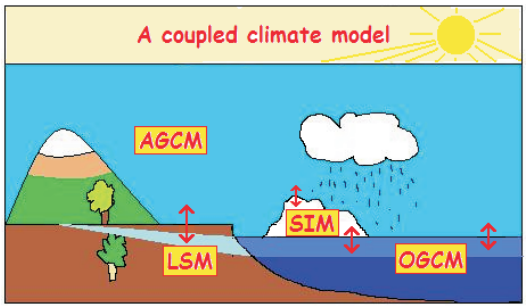

Figure 1.2: *Schematic representation of a coupled climate model, consisting of an Atmospheric General Circulation Model (AGCM), an Oceanic General Circulation Model (OGCM), a Sea Ice Model (SIM) and a Land Surface Model (LSM).*

An LSM describes the processes at the interface between land surface and atmosphere that affect the atmosphere and climate. By calculating the sensible and latent heat and moisture fluxes from the land surface towards the atmosphere, it determines the lower boundary conditions for the heat and moisture equations in the atmosphere. One of the tasks of a LSM is to partition precipitation (obtained from the atmospheric model) into evapotranspiration, surface runoff and water that penetrates into the soil.

In this project, LSMs are assessed by considering simulations of the runoff. The runoff consists of two terms:

1. The drainage, which is generated after infiltration of the water into the soil. It is generated when the water infiltrates through the bottom of the lowest soil layer or when the soil water content exceeds the saturation value in intermediate soil layers. This is a slowly responding term in the hydrological budget, owing to the time needed to propagate the infiltration through the soil column.

2. The surface runoff, which is formed when the infiltration rate exceeds the maximum uptake capacity of the soil. The surface runoff is a fast responding term, which follows changes in the precipitation more directly compared with the drainage.

The runoff formation of two different LSMs, the Tiled ECMWF Surface Scheme for Exchange over Land (TESSEL) and the revised Hydrology Tiled ECMWF Surface Scheme for Exchange over Land (HTESSEL), is considered. The HTESSEL scheme includes some revisions to the soil hydrology. It was developed to improve the formation of surface runoff, because experiments were demonstrating that the TESSEL scheme produces too little surface runoff (Nijsen et al., 2003 and Boone et al., 2004). The revisions included in the HTESSEL scheme consist of the use of a spatially varying soil type and a mapped topography. Also alternative soil hydraulic parameterizations were used (see chapter 2). These features are influencing the soil infiltration capacity and thereby the surface runoff generation: whereas the TESSEL scheme hardly ever produces surface runoff (instead all the water penetrates into the soil), the HTESSEL scheme will always transfer a part of the precipitation to surface runoff.

1.3 Research questions and motivation

For modeling and predicting global climate, a realistic representation of land surface processes is essential. It is therefore important to have an effective method available to validate the behavior of LSMs in global climate models (GCMs).

A routinely used validation method is to force the LSM with observed atmospheric data (such as radiation, rain, temperature and wind) and compare simulated vertical fluxes of energy and water (that is in the form of evaporation) with observations. Scientists who have validated land surface schemes in this way are for instance Henderson-Sellers and Dickinson (1992) [7] and Henderson-Sellers et al. (1996) [6]. However, these point measurements of atmospheric fluxes are not globally available and give only limited insight into the performance of the land surface models at large spatial scales.

Another, maybe more attractive, variable that is regularly used to assess the behavior of LSMs, is the streamflow of water through rivers. River discharge is relatively easy to measure. It is also a spatial integrator of hydrological processes, and gives therefore much insight into the surface water balance at large spatial scales (that is at the scale of river basins). In most land surface schemes, however, the runoff is not routed through rivers (instead, runoff appears in the ocean immediately after its formation). To use streamflow observations for the validation of LSMs, it is therefore necessary to use a specialized river routing model that translates modeled surface runoff and drainage (both defined as a flux of water per unit area) into observable river discharge (which is defined as the runoff, originating from upstream areas, that passes a specific point during its journey towards the ocean; see figure 1.3). For the validation process it is then of crucial importance that the errors in the simulated river discharges, introduced by the river routing model, are small compared to the errors made by the land surface models. Studies that use streamflow for the validation of LSMs are for example performed by Nijssen et al. (1997) [10], Chapelon et al. (2002) [2], Decharme and Douville (2007) [3], Balsamo et al. (2009) [1] and Pappenberger et al. (2009) [11].

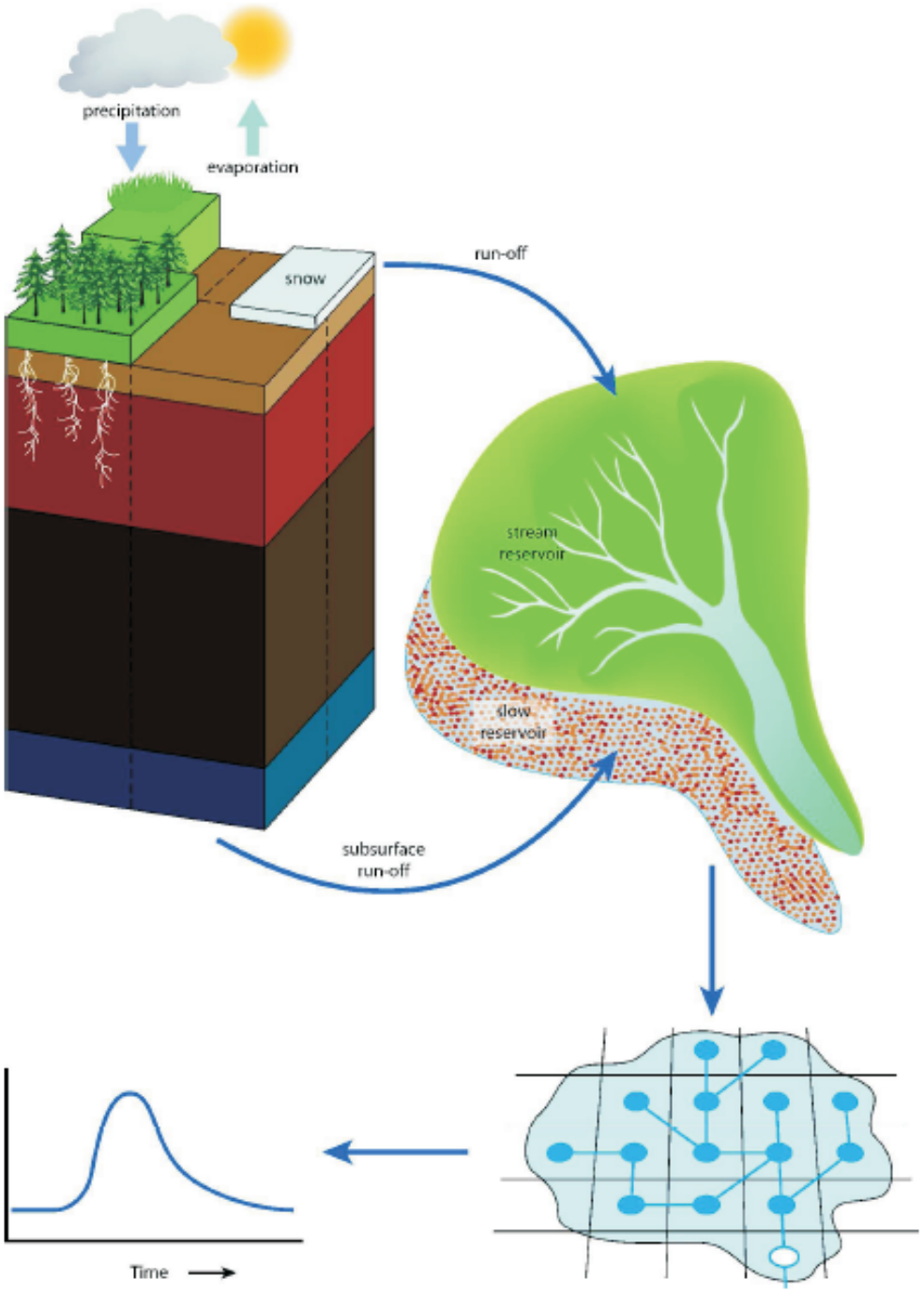

Figure 1.3: *This figure schematically represents a land surface model and a river routing model, which together can simulate river discharges. Pappenberger et (2009) [11].*

Nearly all validation studies and experiments that have been performed consider only stand-alone or offline configurations of the LSMs, in which the LSMs are not coupled to a climate model, but are forced with atmospheric observations. However, it is an essential step in the validation process to consider LSMs that are fully coupled to a climate model (The Project for Intercomparison of Land-surface Parameterization Schemes; PILPS [6]). Furthermore, most studies consider only monthly runoff values and therefore do not assess the daily variability of the simulated runoff.

In this study, the use of the river routing model Total Runoff Integrating Pathways (TRIP) for validating land surface models is discussed. The first question addressed in this thesis is: *What is the usefulness of* TRIP *for the validation of land surface schemes in global climate models (*GCMs*)?* It is hypothesized here that, in comparison with unrouted translation methods, TRIPs translation of runoff into observable river discharge improves the ability to compare the modeled runoff with observations and to assess the LSMs in terms of runoff. This especially concerns the assessment of the short term averages and variances of the modeled runoff (that is, at the time scale from days up to a few months).

Furthermore, an attempt is made to compare and validate the two land surface models Tiled ECMWF Surface Scheme for Exchange over Land (TESSEL) and the revised Hydrology Tiled ECMWF Surface Scheme for Exchange over Land (HTESSEL). Thus, a second main questions addressed in this thesis is: *which of the two schemes ,* TESSEL *or* HTESSEL*, behaves better in terms of runoff modeling?* The LSMs are considered in both offline and online configurations. It is hypothesized that the HTESSEL scheme is better capable to model short term variabilities in the runoff due to the revision of the soil hydrology.

In this study, the climate model EC-EARTH is used to drive the land surface schemes in coupled mode. EC-EARTH is being developed by the KNMI together with a number of other European national weather services (http://ecearth.knmi.nl). It consists of a highly developed atmospheric general circulation model, a highly developed ocean general circulation model, a sea-ice model, a land model (TESSEL or HTESSEL) and an atmospheric chemistry model. The focus of the EC-Earth project is to understand and include the feedbacks between these interacting components as to develop a more comprehensive view of the Earth System than the traditional climate models. One purpose of this study is to get some insight into the behavior of the TESSEL-EC-EARTH and HTESSEL-EC-EARTH combination, including the feedbacks between EC-Earth and the LSMs.

1.4 Outline of thesis

To answer the research questions, the problems are subdivided into multiple subquestions covered in chapter 2 through 8. Chapter 2 describes the land surface models TESSEL and HTESSEL and lists the differences between these models. Some TESSEL and HTESSEL runoff simulations (and their differences) are discussed and two different ways to validate land surface models (offline and online validation) are explained. The TRIP scheme is introduced in chapter 3. To assess the behavior of the TRIP scheme and the errors it introduces, the following experiments are presented in chapter 4 until 7:

- Chapter 4 describes a study on the sensitivities of the TRIP scheme. A simple one dimensional model was constructed, that calculates water balances and water fluxes in the same way as TRIP. With this model, it was possible to regulate changes in the runoff and to monitor the response of the scheme to these changes. Also, parameters as the river width and the river slope could be regulated so that the sensitivities of the output variables to these parameters could be studied in a controlled way.

- In chapter 5, the delaying parameters in TRIP were tuned for the different rivers separately by comparing the timing of the peaks in the discharge simulations with dis-

charge observations (the river discharge data was obtained from the Global Runoff Data Center (GRDC) [15].

- In chapter 6, the effect of the TRIP scheme on discharge simulations of 'real' world rivers was studied by comparing routed discharge with spatially integrated unrouted runoff for the Amazon and Danube river. Therefore, the unrouted runoff was integrated over the drainage area of the rivers. The effect of TRIP on the time series and on the statistics of the river discharge simulations is considered. Also, the influence of some important sensitivity parameters in TRIP was studied. This gives much insight into the kind and the size of the errors in the river discharge that might be introduced by the translation process. For the validation of the LSMs, it is good to know whether the differences between observed and simulated river discharge can be explained by failure of the TRIP scheme or that errors should be ascribed to the LSM.

- To investigate the benefits of TRIP compared with simpler methods for the translation of unrouted runoff into river discharges, the TRIP discharge was compared with discharge estimates obtained by a simple manipulation of the unrouted runoff. This manipulation consists of a shift in time and a moving average to smooth the data. Both, the routed runoff and the manipulated unrouted runoff, were compared with discharge data in chapter 7.

To assess the behavior of the land surface schemes, the following experiments are presented in chapters 7 and 8:

- Offline, unrouted runoff simulations were integrated over the drainage areas of rivers and compared with river discharge observations. Although unrouted runoff can only give rough estimates of the river discharge, it might help to identify large biases in the LSMs.

- Offline discharge simulations of the major rivers on Earth, obtained with the TESSEL-TRIP and the HTESSEL-TRIP combinations, were compared with river discharge data. The time series and statistical quantities as the variance were considered. The differences between observations and simulations were divided into differences that can possibly be explained by failure of the TRIP scheme and differences that can not be explained by errors in the TRIP scheme (and hence, are caused by the LSMs).

- To assess the coupling and feedback mechanisms between the LSM and the atmospheric model, climate simulations were obtained with the EC-EARTH-TESSEL-TRIP and the EC-EARTH-HTESSEL-TRIP combinations. The (statistics of the) online modeled runoff was compared with (the statistics of the) offline runoff simulations (chapter 8). The knowledge about the behavior of the land surface models in a real climate (obtained from offline simulations) was used to assess the performance of the coupled models.

Finally, conclusions, new hypotheses and recommendations are presented in chapter 9.

2

The TESSEL and HTESSEL land surface models

The primary objective of land surface schemes within GCMs is to simulate vertical fluxes of water vapor and latent and sensible heat between land surface and atmosphere. Therefore, runoff is often considered as a by-product. In this project, however, routed runoff is used to assess the two land surface schemes TESSEL and HTESSEL.

In this chapter, the structure of the TESSEL and HTESSEL schemes is described (section 2.1) and the differences between the TESSEL scheme and the revised hydrology land scheme (HTESSEL) are emphasized (section 2.2). Some notes about offline and online validation of the LSMs are included in section 2.3. Finally, TESSEL and HTESSEL runoff simulations (and their differences) are discussed in this section 2.4. The information about the TESSEL and HTESSEL schemes, described in this chapter, is obtained from van den Hurk (2008) [8] and Balsamo et al. (2009) [1].

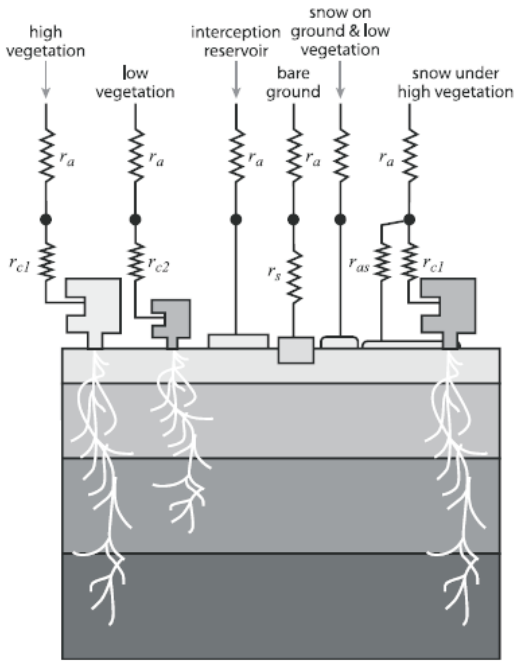

Figure 2.1: *Schematic representation of the structure of the* TESSEL *land surface scheme. Balsamo et al.(2009) [1]*

2.1 The TESSEL hydrology

In the Tiled ecmwf Surface Scheme for Exchange over Land (TESSEL), the global land surface is described on a grid. Each grid-box is divided into fractions (tiles), with up to six fractions over land (bare ground, low and high vegetation, an interception reservoir (that is a thin layer of water on top of the soil/vegetation, collecting liquid water by the interception of rain), shaded and exposed snow) and up to two fractions over water (open and frozen water). Each fraction has its own characteristics, as surface albedo (i.e. the extent to which the surface diffusely reflects light from the sun) and surface roughness (which is a measure of the texture of the surface, which influences turbulence in the lower atmosphere) and defines separate heat and water fluxes. Therefore, for each fraction, the surface energy balance equation (equation 2.1) is solved separately.

Over land, the soil is vertically discretized in four layers. For each layer, the soil temperature and soil moisture is defined at its center. Heat and moisture fluxes are calculated at the interfaces between two adjacent layers. The tessel scheme is shown schematically in figure 2.1.

The stepping procedure

At each time step, a mathematical model performs multiple calculations in a specific, fixed order. The procedure of succeeding actions and calculations (all performed within one time step) by a mathematical model is here called the stepping procedure. The stepping procedure of the tessel scheme is as follows:

1. **Determining land surface characteristics.** Many surface characteristics (as the coverage of snow or the interception reservoir) vary in time and must be updated at every time step. Therefore, at each time step, changes in the surface characteristics are calculated first. At each grid, the presence of the different tiles and the coverage of each tile is determined. Parameters that depend on the land type (as the surface albedo, roughness length e.g.) are defined. The surface characteristics depend on quantities obtained from the atmospheric model and on the state of the land surface (that is the soil temperature and soil moisture). These state variables are updated by the final calculations at each time step (see step 4 of the stepping procedure).

2. **Calculation of the vertical fluxes.** The next step is to calculate the energy fluxes and the rate at which water is extracted by canopy transpiration or bare ground evaporation. The fluxes are found by solving the energy balance equation at the surface:

$$R_n = H + \lambda E + G_s. \tag{2.1}$$

Here R_n is the net incoming (shortwave and longwave) radiation at the surface, which is partitioned into a sensible heat flux H, a latent heat flux λE and the soil heat flux G_s. The components of the energy balance are parametrized as follows:

$$R_n = (1-\alpha)\, K\downarrow + L\downarrow - \epsilon \cdot \sigma \cdot T_s^4 \tag{2.2}$$

$$H = \rho \cdot C_H \cdot U \left(C_p \cdot T_a + gz - C_p \cdot T_s\right) \tag{2.3}$$

$$\lambda E = \lambda \cdot \rho \cdot C_H \cdot U \cdot (\alpha_a \cdot q_\alpha - \alpha_s \cdot q_{sat} \cdot T_s) \tag{2.4}$$

$$G_s = \Lambda_s \left(T_s - T_{sl}\right)^4 \tag{2.5}$$

where $K\downarrow$ is the incoming solar radiation and $(1-\alpha)\, K\downarrow$ is the reflected solar radiation (α is the surface albedo), $L\downarrow$ is the incoming longwave radiation (which comes from the atmosphere and depends on the vertical temperature profile, the clouds and the vertical distribution of absorbers), ϵ is the emissivity of the earth's surface, σ

is the Stefan-Boltzmann constant, T_s is the surface temperature, ρ is the air density, C_H is the aerodynamic turbulent transfer (expressing the efficiency of the transport of heat or moisture away from or towards the surface by turbulent mixing; C_H is calculated by using the Monin-Obukhov similarity theory, which relates turbulent fluxes to atmospheric vertical gradients of temperature, specific humidity and wind speed), U is the horizontal wind speed, C_p is the heat capacity of air, $C_pT_a + gz$ is the dry static energy of the atmosphere, λ is the latent heat of evaporation, α_a and α_s are the atmospheric and surface moisture conductances; α_a and α_s are related to the aerodynamic turbulent transfer C_H, the Leaf Area Index and vegetation type via an other empirical formulation (the Leaf Area Index and vegetation type were calculated in the previous step of the stepping procedure), q_a is the atmospheric specific humidity and q_{sat} is the saturated specific humidity, Λ_s is the soil heat and conductance T_{sl} is the temperature of the top soil layer.

These equations require atmospheric input as atmospheric temperature, humidity, wind speed and incoming short- and longwave radiation. This input is provided by the atmospheric model (or by observations when an offline configuration of the LSM is used). Furthermore, they use surface characteristics (which are predefined in an input file or calculated in the first step) and they depend on the state of the land surface (as the soil temperature and soil moisture). Equation 2.1 is solved first for the surface temperature T_s. The vertical heat fluxes can be found by substituting T_s into equations 2.2, 2.3, 2.4 and 2.5.

As mentioned above, the calculations are performed separately for the different subgrid surface fractions, leading to a separate solution of the surface energy balance equation and surface temperature for each of these tiles. Finally, the fluxes towards the atmosphere from the total grid cells (including all different fractions) are calculated as an area-weighted average over the tiles.

3. **The calculation of the hydrological and thermal fluxes in the soil.** The evapotranspiration of water is calculated by dividing equation 2.4 by the latent heat of evaporation (that is the energy required to evaporate a unit mass of water). Other components of the surface water balance are the runoff of water at the surface and, via the infiltration in the soil, drainage. The last two terms are used in this study to assess the land surface scheme simulations.

   Precipitation is first intercepted by the vegetation and the bare soil, creating an interception layer. This layer accumulates and evaporates precipitation water. When the interception layer is saturated (the amount of water that the interception layer can contain, depends on vegetation and soil type), the remaining precipitation (throughfall) infiltrates into the soil, or, when the upper level of the soil is saturated, it is removed as runoff. Surface runoff is created when a maximum infiltration rate I_{max} into the soil is exceeded. The formulation of surface runoff is:

$$R = T + M - I_{max} \tag{2.6}$$

   where T is the throughfall precipitation and M the snow melt. The throughfall is zero untill the interception layer is full, and equal to the precipitation plus snowmelt afterwards. In TESSEL, the maximum infiltration rate I_{max} is calculated as

$$I_{max} = \rho_w \left[\frac{b_c K_{sat}(-\Psi_{sat})}{\theta_{sat}} \frac{\theta_{sat} - \theta_1}{\frac{z_1}{2}} + K_{sat} \right], \tag{2.7}$$

   where b_c is a scaling parameter, K_{sat}, Ψ_{sat} and θ_{sat} are soil properties at saturation (the value of these parameters should be known for each soil type), z_1 is the depth of

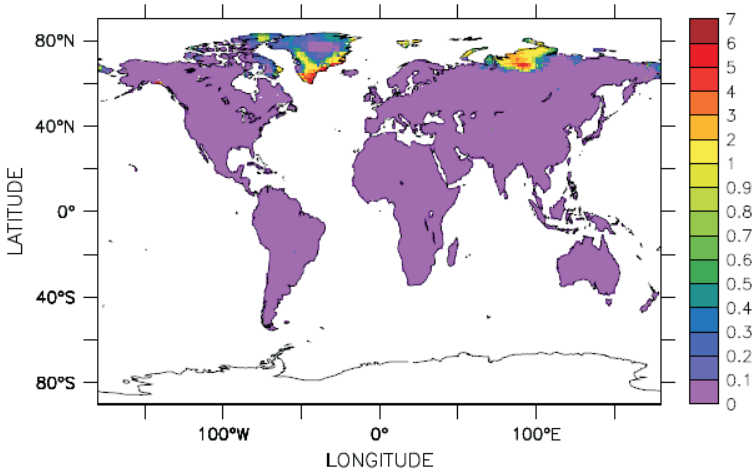

Figure 2.2: *Global plot of the averaged surface runoff (in mm/day) for the northern hemisphere summers (June, July and August) of 1986-1995 as calculated by the* tessel *land scheme in the offline mode (forced with atmospheric observations). The figure shows that* tessel *only produces surface runoff at high latitudes, where frozen soil is present.*

the first soil layer (7 cm in the tessel scheme) and θ_1 is the volumetric water content of the first soil layer (a state variable that is updated at the end of the stepping procedure). This scheme only produces surface runoff in the presence of frozen soil, when infiltration is inhibited, otherwise it hardly ever produces surface runoff (figure 2.2).

In vegetated areas, part of the water that is infiltrated into the soil will be taken up by roots and transpirated back towards the atmosphere. Root extraction is equal to the canopy transpiration (calculated by equation 2.4), divided by the latent heat of evaporation. The water that is not extracted by roots will infiltrate deeper in the soil. The vertical transport of water (caused by a water pressure gradient force and the gravity force) between two subsequent soil layers are calculated by Darcy's law:

$$F_w = -\rho_w \left[D_w \frac{\partial \theta}{\partial z} - K \right] \tag{2.8}$$

where K is the soil hydraulic conductivity (a property of plants, soil or rock, that describes the ease with which water can move through pore spaces or fractures (wikipedia, 2009)) and D_w is the soil hydraulic diffusivity (which governs the fluid flow due to a vertical gradient in the water content). At the surface, F_w is equal to the sum of infiltrating precipitation and melting snow minus bare ground evaporation. At the bottom, free drainage occurs. In the tessel land surface scheme, K and D_w are calculated by using the Clapp and Hornberger (1978) formulation, which is a function of soil water content:

$$D_w = \frac{b_c K_{sat}(-\Psi_{sat})}{\theta_{sat}} \left(\frac{\theta}{\theta_{sat}} \right)^{b_c+2} \tag{2.9}$$

and

$$K = K_{sat} \left(\frac{\theta}{\theta_{sat}} \right)^{2b_c+3}, \tag{2.10}$$

where b_c is a scaling parameter and K_{sat}, Ψ_{sat} and θ_{sat} are soil properties at saturation.

The soil thermal flux at the surface is given by equation 2.5. The vertical heat flux G in deeper layers of the soil is calculated by a simple diffusion equation:

$$G(z) = -D_T \frac{\partial T}{\partial z}, \tag{2.11}$$

where D_T is the thermal diffusivity of the soil (which depends on soil type, of which the vertical distribution might vary). This equation is discretized to calculate the heat flux.

4. **Update of the state variables.** The final calculation in each time step is an update of the state variables (the soil temperature and moisture content within each soil layer). These variables are prognostic variables, whose values change as a result of the surface processes (transport of heat or water, thermodynamic phase change, extraction of water by vegetation, etc.). The prognostic equation for soil temperature is:

$$\rho C_s \frac{\partial T}{\partial t} = -\frac{\partial G}{\partial z}, \tag{2.12}$$

where ρC_s is the volumetric heat capacity of the soil. The boundary condition at the surface is given by equation 2.5 and a zero heat flux is assumed at the bottom. The prognostic equation for soil moisture reads:

$$\rho_w \frac{\partial \theta}{\partial t} = -\frac{\partial F_w}{\partial z} - \rho_w S_R \tag{2.13}$$

with F_w the water flux within the soil (equation 2.8) and S_R is the root extraction by the canopy, which is equal to the canopy transpiration rate (eq 2.4). These equations are discretized to calculate the state variables numerically.

2.2 The H-TESSEL revision

Research revealed some weak components of the TESSEL scheme (see for instance the studies of Nijssen et al. (2003) and Boone et al. (2004)), specifically the lack of surface runoff and the use of a global uniform soil texture. Therefore, a revised land surface hydrology (HTESSEL) has been introduced, which uses new infiltration and runoff schemes with a dependency on the soil texture and standard deviation of orography. In the HTESSEL scheme (figure 2.3), three revisions to the soil hydrology are made:

1. Whereas the TESSEL scheme uses a globally uniform loamy soil texture, in HTESSEL this single soil texture is replaced by a spatially varying soil texture. Six different soil textures are distinguished: coarse, medium, medium-fine, fine, very fine, organic and loamy. For each grid point the dominant soil texture is used. The soil types in HTESSEL are typically of a finer type than the coarse loamy soil in TESSEL.

2. For the calculation of soil hydraulic conductivity G and the soil hydraulic diffusivity D, the Genuchten formulation is used, instead of the Clapp and Hornberger scheme. The van Genuchten formulation for the hydraulic conductivity reads:

$$K = K_{sat} s^l \left[1 - \left(1 - s^{\frac{1}{m}}\right)^m\right]^2, \tag{2.14}$$

where s is the normalized water content, $s = \frac{\theta - \theta_r}{\theta_s - \theta_r}$. The residual water content θ_r is usually defined as the small amount of tightly-bound water remaining in the

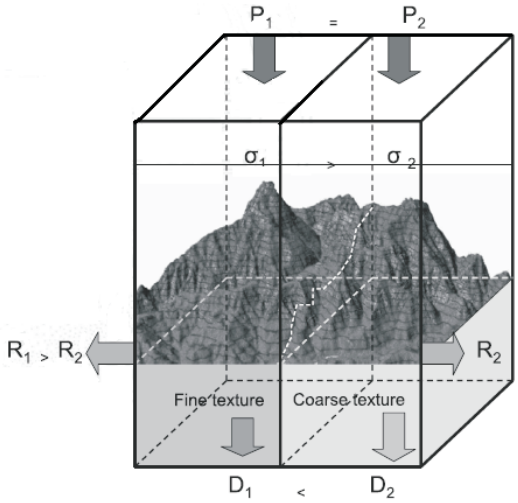

Figure 2.3: *Spatial structure added in H-TESSEL. The distribution of the water into surface runoff and drainage depends on orography and soil texture. Balsamo et al.(2009) [1]*

soil, when the soil has been dried for a long time. The van Genuchten formulation uses more scaling parameters (l and m) than the Clapp and Hornberger formulation and can therefore describe the conductivity more accurate, which is shown by intercomparison studies (Shao and Irannejad; 1990).

3. The surface runoff generation is altered by a variable infiltration capacity which is based on soil saturation and the local variability of the topography. The soil hydraulic conductivity and diffusivity given by the van Genuchten equation for the soil textures in htessel are smaller than those of the tessel scheme (calculated by the Clapp and Hornberger equations), which results in a reduced infiltration of the water and consequently in the generation of more surface runoff. Whereas the tessel scheme hardly produces surface runoff, the htessel scheme will always produce surface runoff, especially in mountains and rocky regions.

2.3 Offline and online validation of LSMs

Land surface models are designed to be embedded in a climate model. The configuration in which a land surface model is fully coupled to a climate model is called the *online mode* (see figure 2.4).

Most validation experiments however, consider lsms in the *offline mode* (also called the stand-alone mode). In the offline configuration, the lsm is decoupled from its host climate model and forced with atmospheric observations. The reason for using the offline configuration is that climate models usually make large errors in estimating and predicting atmospheric quantities as precipitation. When the lsm is coupled to a climate model, it is forced with uncertain atmospheric quantities, which makes it difficult to isolate the behavior of the lsm. For a complete validation however, online simulations (also called climate simulations) are necessary to get insight in the performance and the stability of the total coupled system (The Project for Intercomparison of Land-surface Parameterization Schemes; pilps [6]). Only by online validation, the induced feedback mechanisms for processes in the atmosphere can be assessed.

In this project, both online and offline configurations of the land surface models are used for the validation process. Offline tessel and htessel simulations of the runoff

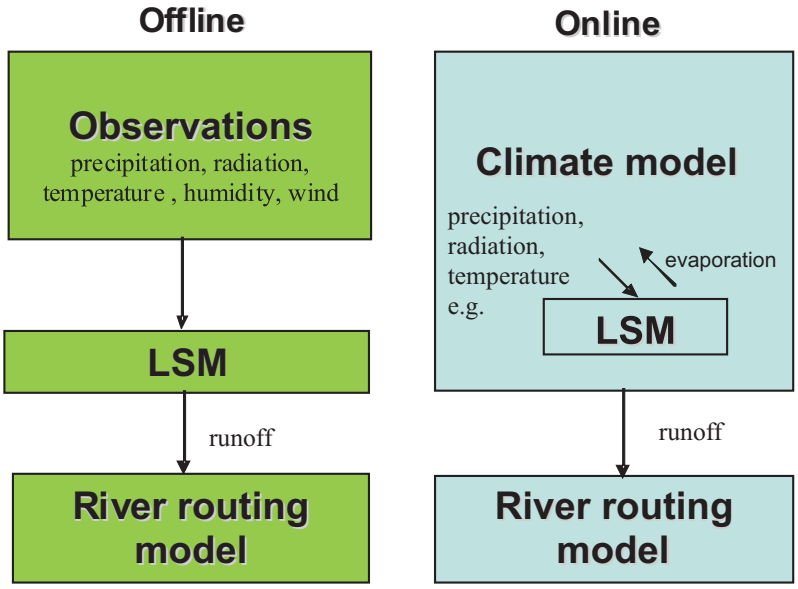

Figure 2.4: *Schematic representations of the offline and online models.*

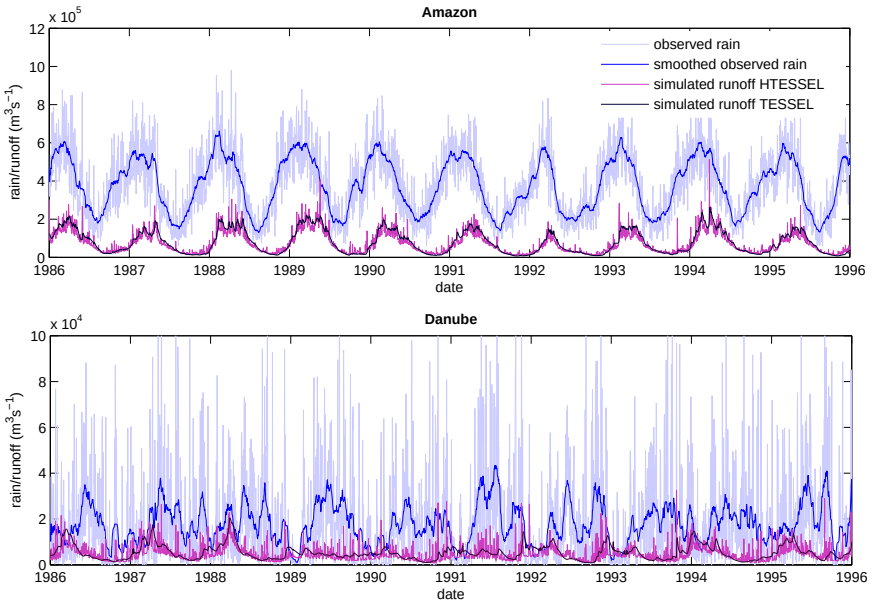

Figure 2.5: *Time series of observed rain (that was used to force the* LSMs*) and time series of offline runoff simulations (performed with* TESSEL *and* HTESSEL *that were forced with atmospheric observations) within the Amazon and Danube river basin. Moving averages (dark blue line) were used to smooth the data as to show the coarse features of the time series. The ticks are placed at the first of January of the indicated year.*

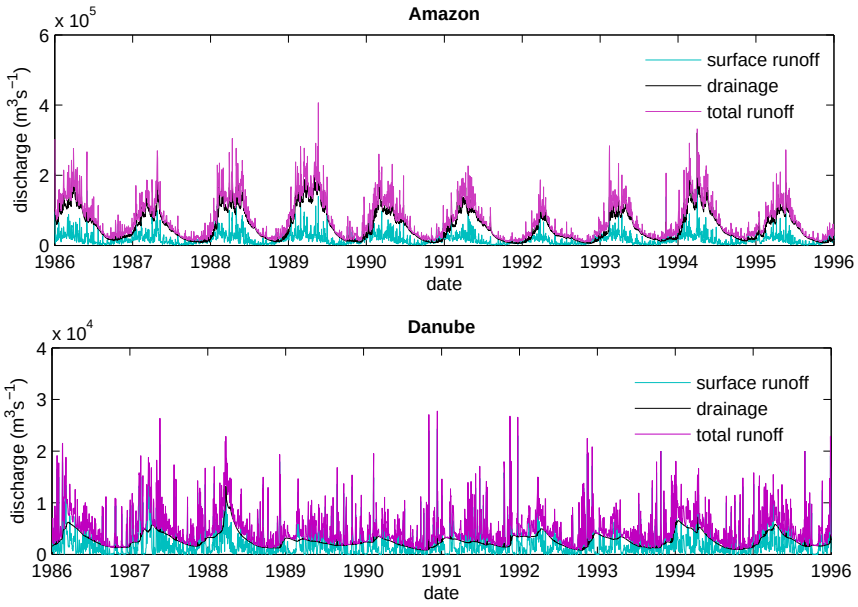

Figure 2.6: *Surface runoff, drainage and total runoff simulated by the* HTESSEL *scheme for the Amazon (top) and Danube (bottom) river. Only the components as simulated by the* HTESSEL *scheme are plotted, since the* TESSEL *scheme barely produces surface runoff (the total runoff is then thus equal to the drainage).*

were obtained from Balsamo et al.(2009), who forced the LSMS with near-surface forcings provided by the second Global Soil Wetness Project (GSWP-2). Climate simulations were performed with climate model EC-EARTH, alternately coupled to the TESSEL or HTESSEL land surface scheme.

2.4 Runoff simulations

Time series of the TESSEL and HTESSEL runoff simulations and the observed rain within the Amazon and Danube basin are plotted in figure 2.5. The figure shows the runoff integrated over the total drainage areas of the rivers.

Concerning the differences between the TESSEL and HTESSEL simulations, figure 2.5 shows that the HTESSEL curves are more variable at small time scales, which indicates a faster process of runoff formation: a considerable large fraction of the HTESSEL runoff is surface runoff (see figure 2.6), whereas the TESSEL runoff only contains drainage (the TESSEL scheme hardly ever produces surface runoff, see chapter 2.1). That the TESSEL and HTESSEL runoff simulations especially differ at small time scales is also shown by figure 2.7, where the relative differences between the TESSEL and HTESSEL runoff are plotted for different averaging times. The HTESSEL scheme produces relatively much surface runoff in the Danube region, compared with the Amazon region (figure 2.6).

To compare runoff simulations with streamflow data, the runoff should first be translated into river discharge. Simulated river discharges are presented and compared with observations in chapter 7.

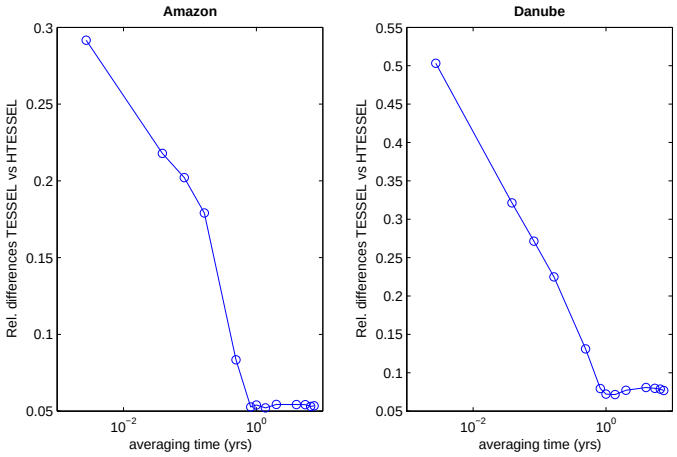

Figure 2.7: *Relative differences between runoff simulations by the* TESSEL *and* HTESSEL *schemes (that is the absolute difference between the runoff obtained with the different schemes, divided by the runoff obtained with the* TESSEL *scheme), averaged over the drainage regions of the Amazon and Danube river and over some time (the averaging time is represented on the x-axis). The* TESSEL *and* HTESSEL *simultions especially differ at time scales of days up to a few months.*

3

Total Runoff Integrating Pathways (TRIP)

The Total Runoff Integrating Pathways (TRIP; Oki and Sud, 1997) is a global river routing model, which can be used to isolate river basins and route runoff to the river mouths for all major rivers on earth. The TRIP model uses a 1^o latitude by 1^o longitude grid on which the drainage areas and flow directions of 180 major rivers on earth, distributed over 63% of land (Antartica and Greenland are excluded) are defined (see figure 3.1).

Because TRIP translates runoff values into measurable river discharges, it provides a method for comparing and validating land surface models. In the following chapters, the use of TRIP for validating LSMs is discussed. But fist, the concept of the TRIP scheme is explained in this chapter.

3.1 The flow routing algorithm

In the TRIP model, the global land surface is divided into gridcells of 1^o latitude by 1^o longitude. Each gridcell contains a surface water (the river) and a groundwater reservoir (figure 3.2). These reservoirs respectively obtain surface runoff and drainage from an input file (these values might for instance be provided by a climate model, a stand alone version of a land surface scheme or by (satelite) observations). A surface reservoir loses water by

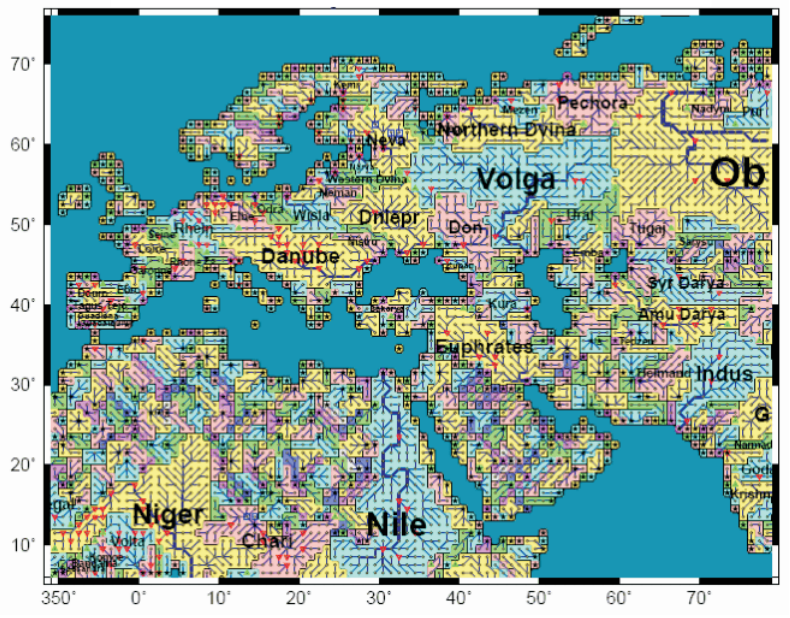

Figure 3.1: *The rivers of Europe on the* TRIP *template ($1^o x 1^o$; Oki and Sud, 1997).*

transferring water to the surface reservoir of the next grid, downstream the river. The flow velocity (and hence the travel time between the grid cells) of the water through the river is estimated by using Manning's equation (equation 3.11). The ground water reservoirs are not connected to each other directly, i.e. water does not leave the grids as groundwater. Instead, a groundwater reservoir loses water by transporting it to the surface reservoir of the same grid (figure 3.2). A certain residence time in the groundwater reservoirs accounts for the delay of the subsurface runoff in entering the river streams. This residence time is roughly considered to be a constant in space and time and must be defined in an input file. The cross-section of the river channel is assumed to be rectangular and the river width is obtained using a geomorphologic relationship between width and annual mean discharge (as discussed in section 3.3).

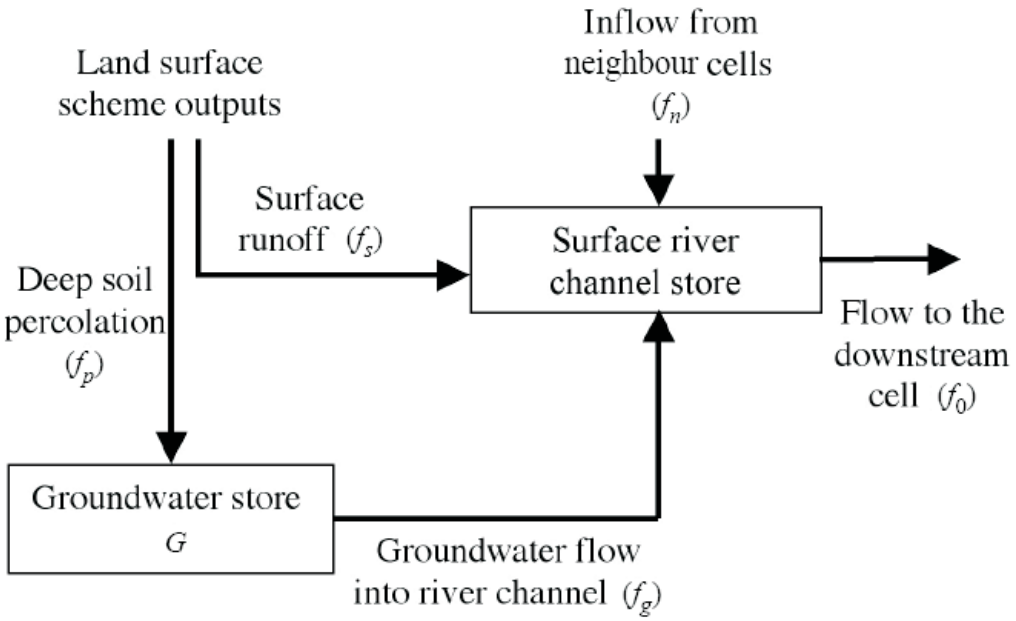

Figure 3.2: *Schematic representation of the flow routing algorithm of* TRIP *and the simple model (Picher et al., 2003) [12].*

To translate runoff (obtained from a LSM) into river discharge, initial conditions of variables as the river storage and the groundwater storage need to be specified. These initial conditions are not measured, but rather calculated before the final simulation is started.

In fact, the TRIP simulation consists of two stages. In the first stage, the *spin up*, initial conditions for the state variables as the river storage and the groundwater storage are derived. For this end, the river routing model is repeatedly forced, for instance, with data of only the first year of the full time series. The state variables are initially arbitrarily chosen, but during the multiple runs of the spin up the state variables are updated. During the spin up, the initial values of each new run are set equal to the simulated state variables at the end of the previous run. This goes on until the values of the state variables at the end of the simulation year are in agreement (within a given percentage) with the values obtained after the previous run (for the simulations in this project, the spin up was ended when the state variables at the end of two successive years was smaller than 5%). In a second stage, the full time series of the runoff is applied to the reservoirs and river discharges are calculated and written in an output file.

3.2 The input

To run TRIP, some parameters have to be specified in an input file. Some parameters are globally uniform: the residence time in the groundwater reservoirs, the meandering ratio, parameters (a, b, c and d) to calculate the Manning's coefficient (equation 3.12), a minimum river width and values for the initial river storage and groundwater storage (these can be chosen arbitrary when a spin up is performed before the final calculations). Furthermore, the TRIP scheme requires global maps on which the flow directions, elevations and river sequences (a numbering of the grid points within a drainage area, starting with the lowest numbers at the river source and increasing when following the rivers to the mouth) are defined for each grid box. The TRIP scheme uses a time series of daily runoff and drainage values (for instance obtained from a land surface model) to calculate river discharges.

3.3 Stepping procedure

The task of the TRIP model is to read a time series of global (daily) runoff values (obtained from a LSM) and to translate this into a time series of global (daily) river discharge. To fulfill this task, succeeding actions and calculations are performed by the TRIP model at each time step (the time step length is equal to a day, when daily runoff values are used). These succeeding actions and calculations are described in this section.

The outflow groundwater discharge

The outflow of groundwater from the groundwater reservoir into the river channel (within a given grid), is obtained from the water balance equation. The water balance of a ground reservoir G is determined by the drainage input f_p into and the outflow groundwater discharge f_g from that reservoir,

$$\frac{dG}{dt} = f_p - f_g. \tag{3.1}$$

The outflow discharge is assumed to be a linear function of the groundwater storage, $f_g = \frac{1}{\tau_g} \cdot G$, where τ_g is the residence time in the groundwater reservoir (specified in the input file). Substitution of f_g into equation 3.2 yields:

$$\frac{dG}{dt} = f_p - \frac{1}{\tau_g} \cdot G. \tag{3.2}$$

Taking f_p constant (within one time step), the following solution can be obtained (text box 3.3):

$$G(t) = f_p \cdot \tau_g + \left(G_0 - f_p \cdot \tau_g\right) \cdot e^{-\frac{1}{\tau_g} \cdot t}. \tag{3.3}$$

Discretization yields the following expression:

$$G_{t+\Delta t} = G_t e^{-\frac{1}{\tau_g} \cdot \Delta t} + \left(1 - e^{-\frac{1}{\tau_g} \cdot \Delta t}\right) f_p \cdot \tau_g. \tag{3.4}$$

The outflow groundwater discharge between time t and $t + \Delta t$ is then given by:

$$f_g = f_p - \frac{G_{t+\Delta t} - G_t}{\Delta t}. \tag{3.5}$$

The river discharge

The river discharge from a given grid is calculated by using the water balance in the surface reservoir, which is determined by the inflow I into and the outflow Q from the reservoir,

$$\frac{dS}{dt} = I - Q, \tag{3.6}$$

where S is the river storage. The inflow consists of surface runoff generated within the grid cell (f_s), the inflow from the upstream grid (f_n), and the outflow from the groundwater storage of the same grid (f_g):

$$I = f_s + f_n + f_g. \tag{3.7}$$

The outflow discharge is assumed to be a linear function of the storage, $Q = \frac{1}{\tau} \cdot S$, where τ is the travel time between the grid cell under consideration and its downstream neighbor, i.e. $\tau = \frac{L}{V}$ with L the distance between the grid cells and V the flow velocity. When this is substituted for Q into equation 3.6, and the inflow is assumed to be constant (during one time step), the following solution is obtained (textbox 1):

$$S(t) = S_0 \cdot e^{-\frac{V}{L} \cdot t} + \left(1 - e^{-\frac{V}{L} \cdot t}\right) \cdot I \cdot \frac{L}{V}, \tag{3.8}$$

which yields the following relation between the storage S_t before and the storage $S_{t+\Delta t}$ after a time step Δt:

$$S_{t+\Delta t} = S_t e^{-\frac{\Delta t \cdot V}{L}} + \left(1 - e^{-\frac{\Delta t \cdot V}{L}}\right) \cdot I \cdot \frac{L}{V}. \tag{3.9}$$

The expression for the river storage consists of two terms. The first term represents the amount of the stored water at time t that is still left in the reservoir at time $t + \Delta t$. The second term is the part of the runoff, obtained during time Δt, that is still left in the reservoir at time $t + \Delta t$, i.e. $\int_t^{t+\Delta t} I(t) \cdot e^{-\frac{V}{L} \cdot t} dt$. When the inflow is constant in time, the storage approaches an equilibrium in which

$$S = \frac{L}{V} \cdot I. \tag{3.10}$$

The flow velocity of the surface water in the river channel is calculated with Manning's equation,

$$V = \frac{1}{n} R^{\frac{2}{3}} s^{\frac{1}{2}}, \tag{3.11}$$

where n is the Manning's roughness coefficient (also called hydraulic resistance), R is the hydraulic radius (cross section area of the river divided by the wetted perimeter) and s is the slope of the river channel. Manning's roughness coefficient n is calculated using an equation developed by Dingman and Sharma (1997)[4]:

$$n = \frac{1}{1.564} \cdot A^{-0.173} \cdot R^{0.267} \cdot s^{0.5 + 0.0543 \cdot \log(s)}, \tag{3.12}$$

where A is the cross sectional area of the river ($A = Wh$). Substitution of n into equation 3.11 yields for the flow velocity:

$$V = 1.564 \cdot (W \cdot h)^{0.173} \cdot \left(\frac{W \cdot h}{W + 2h}\right)^{0.4} s^{-0.0543 \cdot \log(s)} \tag{3.13}$$

where h is the river depth given by

$$h = \frac{S}{W \cdot M_r L}, \tag{3.14}$$

W is the river width (determined by a geomorphologic relationship between width and the mean annual discharge, see equation 3.16) and M_r is the meandering ratio (which accounts for the meandering of the river channels within a grid cell). The river width is obtained using a geomorphologic relationship (Philippe Lucas-Picher et al., 2002 [12]) between the mean annual discharge (Q_m,m^3s^{-1}) passing through a river section and river width (W,m):

$$W = max\left(W_m, Z\sqrt{Q_m}\right) \tag{3.15}$$

$$Z = \left(10^{-4}Q_{m,mouth} + 6\right), \tag{3.16}$$

where Q_m is the annual mean discharge passing through a river section and $Q_{m,mouth}$ represents Q_m at the river mouth. Geomorphologic relationships between width and discharge are discussed in geomorphologic literature (for instance by Leopold et al. (1964) [9] and Richards (1987) [13]).

The outflow discharge between time t and $t + \Delta t$ is then calculated by:

$$Q = I - \frac{S_{t+\Delta t} - S_t}{\Delta t} \tag{3.17}$$

Equation 3.2 and 3.6 are inhomogeneous differential equations. The solution of this kind of equations is given by the sum of the solution of the homogeneous equation and a particular solution of the inhomogeneous equation. For the groundwater storage, the homogeneous equation is

$$\frac{dG}{dt} = -\frac{1}{\tau_g} \cdot G, \tag{3.18}$$

and its solution

$$G(t)_{hom} = C \cdot e^{-\frac{1}{\tau} \cdot t}$$

A solution of the inhomogeneous equation is

$$G(t)_{par} = f_p \cdot \tau$$

and the general solution is thus found to be

$$G(t) = f_p \cdot \tau_g + C \cdot e^{-\frac{1}{\tau_g} \cdot t}. \tag{3.19}$$

where $C = G_0 - f_p \cdot \tau_g$ ($G_0 = G(0)$). It is now easy to derive the relation between $G(t)$ and $G(t + \Delta t)$:

$$G_{t+\Delta t} = f_p \cdot \tau_g + \left(G_t - f_p\tau_g\right) \cdot e^{-\frac{1}{\tau_g} \cdot \Delta t}.$$

The solution for the river water storage $S(t)$ can be found in a similar way.

4

A study of the sensitivities of TRIP

When TRIP is used for the validation of land surface models, it is of crucial importance that the errors introduced by the river routing model are small compared to the errors made by the LSM or, otherwise, that the errors of different sources (TRIP versus the LSM) can be distinguished from each other. As a first step to understand the behavior of the TRIP model and to study its sensitivities and errors, a simple, one dimensional, model was constructed that calculates water balances and water fluxes in the same way as TRIP. With this model, it was possible to regulate changes in the runoff and to change parameters as the river width and the river slope. The model was used to study the way output variables depend on and are sensitive to the most important sensitivity parameters in TRIP.

In section 4.1 the simple model is described. In section 4.2, the step response of the river storage, flow depth, flow velocity and river discharge is plotted for different values of the river slope, the river width, the groundwater parameter and the fraction of surface runoff and drainage. Results are explained and discussed. Conclusions are drawn in chapter 4.3.

4.1 The design of the model

The simple model calculates water balances and water fluxes in the same way as TRIP (using the same equations), but it is one dimensional and consists of only 10 grid points, representing an imaginary river (see figure 4.1). Each grid contains a surface water reservoir (the river) and a groundwater reservoir (figure 3.2), that respectively obtain surface runoff and drainage from an input file. The delivered runoff values are not real measured or modeled runoff values. Also, the values for the ground elevations and river slopes are just imaginary and do not represent a real area on earth. However, the values of the variables (river slope, runoff values etc.) are realistic and might occur in the real world. The scheme of the simple river model consists of ten grids, pursuing the river to its mouth

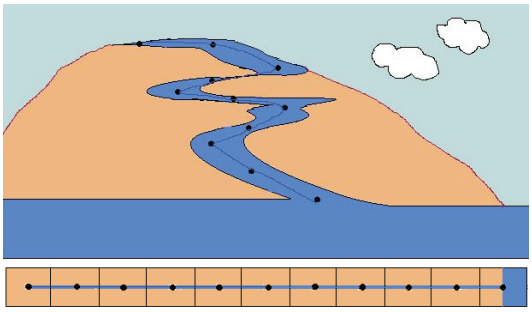

Figure 4.1: *schematic representation of a river on a hill*

(see figure 4.1). As the TRIP simulations, a simulation with the simple model consists of

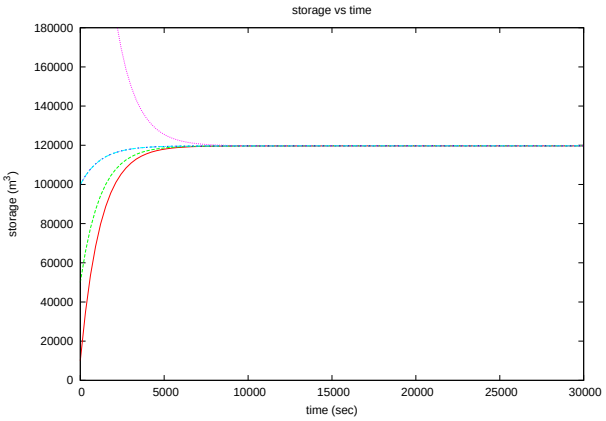

Figure 4.2: *Evolving river storage in time for a constant inflow in a specific river basin, starting from different initial values. The equilibrium value that is reached after some time does not depend on the initial value. Instead, it does depend on properties of the system as river slope, river width and the amount of inflow.*

two stages. A spinup is performed first, in which a balance is obtained in each reservoir between the inflow (consisting of the runoff and drainage within a specific grid cell, specified in an input file, plus the inflow from upstream grid cells) and the outflow of water from that reservoir (see figure 4.2). In a second stage, the runoff and drainage forcings are changed for some time (called the *runoff pulse* and *drainage pulse* hereafter), bringing the system out of balance.

The input file

In an input file the following uniform parameters are specified which were the same for each grid cell: the time step length, the length of the grid cells, the surface area of the grid cells, the river slope in the grids, the width of the river, the residence time in the groundwater reservoirs, the values of initial river storage and groundwater storage and the daily runoff and drainage values for which a balance was obtained first. For the first grid cell, also the size of the runoff and drainage pulses were specified.

The stepping procedure

At each time step, a mathematical model performs multiple calculations in a specific, fixed order. The procedure of succeeding actions and calculations by the model (all performed within one time step) is called the stepping procedure. The stepping procedure of the simple model is as follows:

1. For the first calculations, the initial river storage and groundwater storage (specified in the input file) and equation 3.4, are used to calculate the groundwater storage after the first time step for each grid. Equation 3.5 is used to obtain the outflow groundwater discharge during that time step.

2. For each grid, the water level height is calculated by dividing the initial storage by the river width (in this model, the river width at each grid point is assumed to be constant in time and is specified in the input file). Then, equation 3.13 is used to calculate the surface river channel flow velocity. The initial storage and groundwater storage and the calculated water level height and flow velocity are written in an output file.

3. Then a calculation is done for the first grid alone: the inflow (equation 3.7), the river storage after the first time step (equation 3.9) and the outflow discharge of the river during the first time step (equation 3.17) are calculated. For the first grid the inflow from the upstream cell (f_n) is set to zero. The inflow and discharge are written in an output file.
4. The discharge Q of the first grid is set equal to the inflow from the upstream cell, f_n, of the second grid.
5. Step 3 and 4 are repeated for all grids.
6. The initial storage and groundwater storage of each grid are replaced by the storage and groundwater storage after the first time step:

$$S_{t+\Delta t} \rightarrow S_t,$$
$$G_{t+\Delta t} \rightarrow G_t.$$

7. Step 1 until step 6 are repeated for all time steps.

4.2 Results and discussion

With the simple model, a river was simulated which experiences a period of constant runoff and in which an equilibrium is established that suits that specific amount of runoff. Then, at once, the river experiences a change in the runoff (representing for instance a small period of heavy rain fall).

The model has been run for different values of the runoff pulse, the river slope, the river width and the residence time in the groundwater reservoir. In all situations, the outflow discharge was first brought into balance with a given amount of runoff and drainage at each grid cell. When a balance was obtained, a runoff and/or a drainage pulse was applied to the first grid cell of the system, while the other grid cells were still obtaining the 'normal' amount of runoff and drainage. The evolution of the river storage, depth, velocity and outflow discharge after the change in runoff is monitored. The step response of the system is studied. Since the system is linear (see figures 4.3 and 4.4) and time independent, the step response gives enough information to determine the behavior of the system for other input signals (the response on an arbitrary input signal can be obtained by convolution of the input signal and the impuls response of the system. The impuls response is directly related to the step response). In most figures that are presented in this report, the variables are plotted for the first grid alone. In figures 4.7 and 4.9, the output variables are also plotted for grid cells downstream the river.

The sensitivity to pulse size

Figures 4.3 and 4.4 show the river storage, flow depth, flow velocity and river discharge for different runoff values. The figure shows that the peak in the runoff results in a peak in all output variables. When a runoff pulse is applied, the amount of inflow will increase suddenly, but the outflow discharge will not follow this increase immediately. Instead, a part of the incoming water is stored in the reservoir, increasing the reservoir storage and flow depth (equation 3.9). The flow depth directly influences the flow velocity via the wetted perimeter and the cross section of the river (equation 3.13). The increased inflow, together with the change in river storage, alters the outflow discharge via equation 3.17. All variables (storage, depth, velocity and discharge) respond approximately linearly to the size of the runoff pulse.

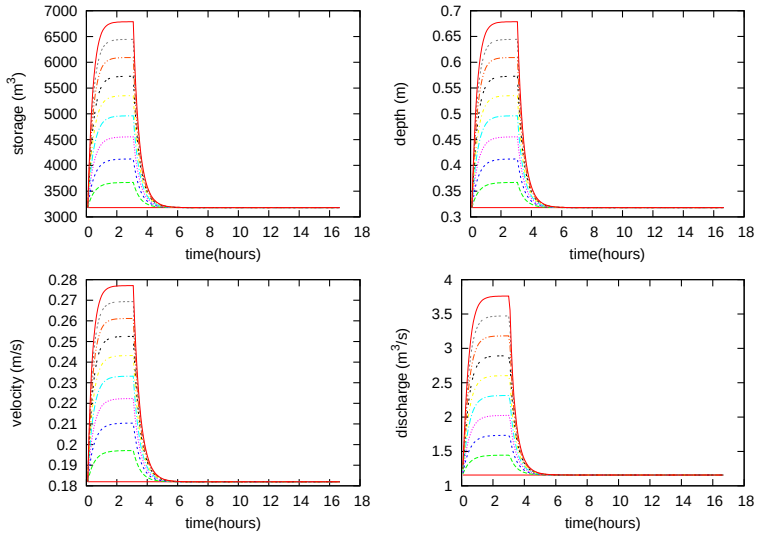

Figure 4.3: *Model output. The evolution of the storage, depth, velocity and discharge after a three hours during surface runoff pulse was applied from t=0 onwards. Different colors indicate different pulse sizes (ranging from 1 to 10 times the spin up value). The drainage supply was constant. The slope was* 10^{-4} *for all curves. The system is said to be (approximately) linear, because the response of the system increases (more or less) linearly with the amount of (surface) runoff. The new equilibrium values are determined by the climatological value of the drainage plus the new values of the surface runoff.*

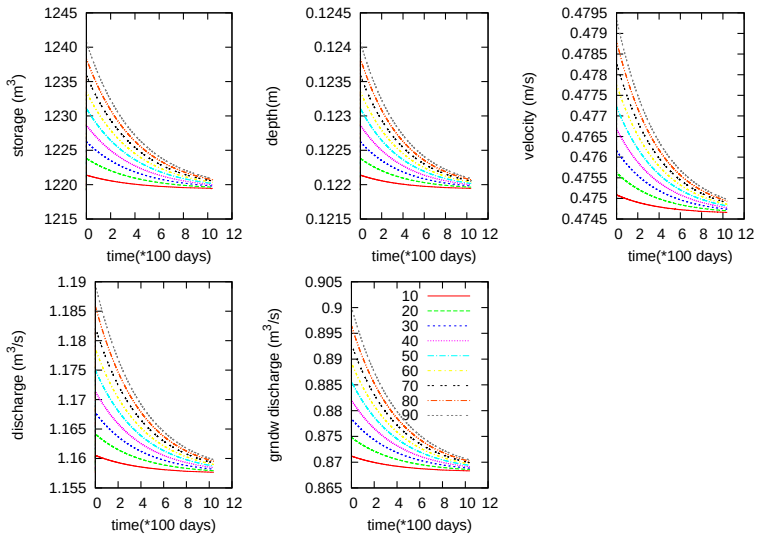

Figure 4.4: *Model output. The evolution of the storage, depth, velocity and discharge after a drainage runoff pulse was applied on* $t = 0$*. The surface runoff was constant. Different colors indicate different pulse sizes (ranging from 1 to 90 times the spin up value). The slope was* 10^{-4} *for all curves. Notice that the system reacts very slowly on the drainage pulses and that the changes in the output variables due to these pulses are much smaller than the changes in figure 4.3. The drainage is much more influencing the long term average. Note that the three hours during time pulse at* $t = 0$ *is far too short to obtain a new equilibrium.*

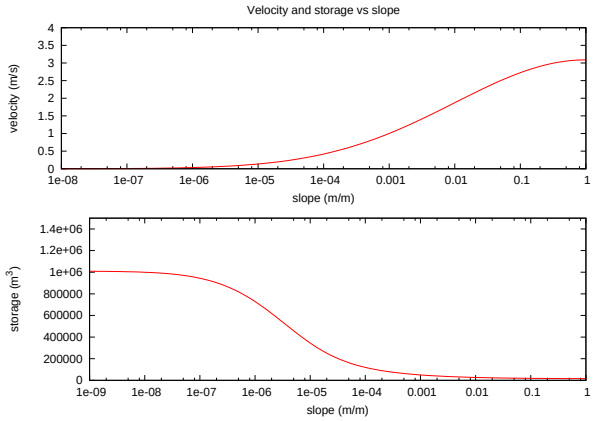

Figure 4.5: *The flow velocity and river storage plotted versus the slope of the river channel. This relation is obtained from the Manning formula. All other parameters in this equation are taken constant.*

The sensitivity to the river slope

The river slope most directly influences the flow velocity. The stream flow is driven by gravity and described by the empirical Manning formula (equation 3.13), which depends on the vertical slope of the river. The flow velocity in the channel is an important variable, since it determines the velocity with which a disturbance is traveling through the river. It also determines the typical time scale at which the system, at a given point, adjusts to a change in the inflow. An excess of water is faster transported out from a grid cell when the flow velocity is large (the exponential terms in equation 3.8 are describing a more rapid decay for large flow velocities). The relation between the velocity and river slope, calculated by the Manning formula, is plotted in figure 4.5. Large river slopes result in high flow velocities. This is also in agreement with the model results (figures 4.6 and 4.7). Figure 4.6 indicates that, for the plotted slopes, the velocity tends to increase logarithmically with the river slope to base 2 (doubling the river slope results in a linear increase in the flow velocity). An error of 100% in the river slope results here in an error of about $0.05 m/s$ in the equilibrium values of the flow velocity (for the plotted range in slopes), which is an error between 10% and 25%. This is more or less in agreement with figure 4.7, which indicates that a change in the river slope of 100% results in a change in the travel time of about 10 (large slopes) to 60 minutes (small slopes) over a distance of 5 km. To simulate a realistic time series of river discharge, it is thus important that the error in the river slope is small. Since the grid that is used by TRIP (of 1 by 1 degree) is quite coarse to define the slopes on, errors in the defined river slope might cause large errors in the flow velocity and the total travel time of the water.

Via its effect on the flow velocity, the slope also has an effect on the river storage and river depth. For a larger flow velocity, an equilibrium between the inflow and outflow discharge will be obtained faster, leading to a smaller river storage and flow depth. Equations 3.10 and 3.14 indicate an inversely proportional relation between flow velocity and river storage and flow depth (in equilibrium state). An error of 100% in the river slope will result in an error of about 10% to 20% in the river depth for the slopes indicated in figure 4.6.

Figure 4.6 indicates that also the (absolute) effect of a runoff pulse on the output variables depends on the slope of the river. A larger slope will lead to a large response of the flow velocity, storage and river depth to a runoff pulse. The dependency of the response of the flow velocity on the river slope can be explained by equation 3.13; the flow velocity directly depends on the river depth, via the wetted perimeter and the cross

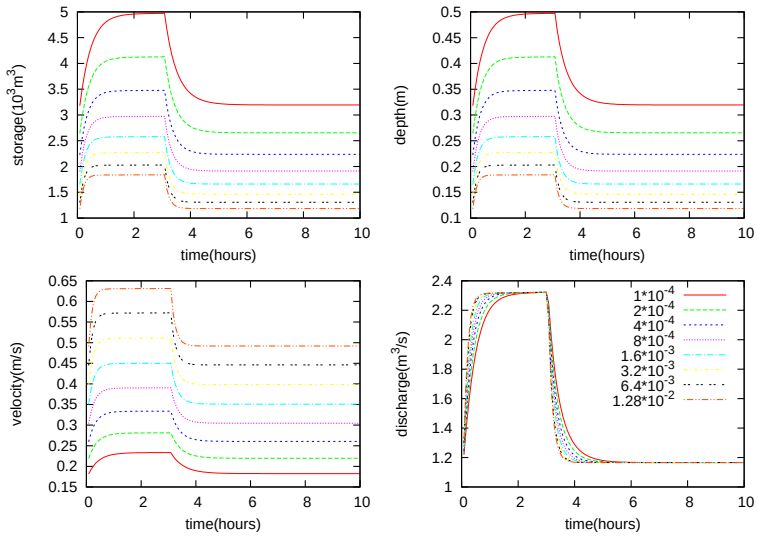

Figure 4.6: *Model output: Evolution of the river storage, flow depth, flow velocity and river discharge in the first grid. A 3 hour during runoff pulse and drainage pulse, of both 5 times the spin up values, is given simultaneously, starting at t=0. Different colors indicate different river slopes (ranging from* 10^{-6}*(red) to* 10^{-2} *(gray)).*

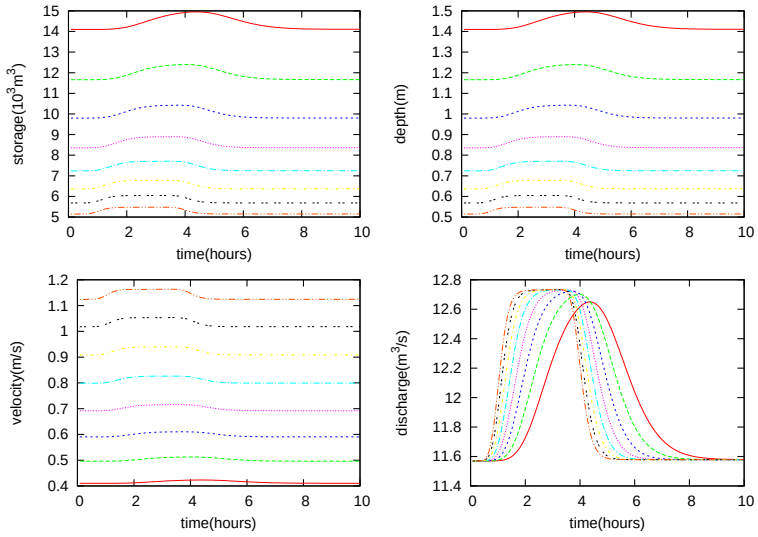

Figure 4.7: *Model output: The same as figure 4.6 but now at a distance of about 5 km from the disturbance.*

section of the river. These terms are multiplied with a factor $s^{-0.0543 \cdot log(s)}$, which induces a dependency of the response on the slope of the river. The response of the river storage and flow depth to a runoff pulse is larger for small river slopes. This is because, in case of a large flow velocity (large slope), the outflow discharge can follow a change in the inflow more directly, so that less water is stored in the reservoir as a consequence of the difference between the amount of inflow and discharge. The relative effect of a runoff pulse on the output variables is less sensitive to the river slope. The pulse causes an increase in the river storage and flow depth of about 55% and the flow velocity increases with about 30% due to the runoff pulse, for all indicated river slopes.

An important difference between the outflow discharge and the other variables (storage, flow velocity and depth) is that when the system is in balance (at time zero and after 6 hours in figure 4.6), the outflow discharge does not depend on the river slope. This is because the outflow discharge of a system that is in balance, is fully determined by the inflow (since the outflow is precisely equal to the inflow in case of equilibrium). However, when the amount of inflow changes, there is an unbalance between the inflow and the outflow discharge. The way the outflow discharge adjusts to obtain a new balance, is influenced by parameters as the slope of the river channel. When the slope is large, much of the inflow is transported out of the grid right away. The part that is temporally stored in the reservoir will decay on a short time scale. Therefore, large inflow will very soon result in a large outflow discharge and when the inflow is normal again, the old balance is re-obtained in little time (gray and the dashed red line in the lower right panel in figure 4.6). For smaller river slopes, the adjustment process is slower. In first instance, an increase in the surface runoff will result in an increase in the river storage (the second term in equation 3.9 is large for small flow velocities). The increased river storage will suppress the increase in outflow discharge (since it results in a positive numerator in the second term of equation 3.17). When the pulse has ended, the discharge is decreasing again (since the first term in equation 3.17 is small), but the part of the stored water that is still in the reservoir, is decaying slowly and keeps the outflow discharge large for a long time (the numerator in equation 3.17 is negative now). When, long after the pulse is applied, all systems are in balance again, the total amount of discharged water is the same for all systems (the area under the different colored curves in the lower left panel of figures 4.6 and 4.7 is equal). This amount is equal to the total amount of inflow during that time.

Figure 4.7 indicates that the pulse is spread out in space and time when the water is traveling downstream the river. This can be explained by the storage capacities of the reservoirs. During equilibrium, the inflow into a reservoir is equal to the outflow discharge from that reservoir. When a runoff pulse is applied, the outflow discharge will not immediately be as large as the inflow (since the flow velocity does not change immediately) and the storage of the reservoir increases. The water that is stored in a reservoir will be transported to the next grid via an exponential decay. This process is more extended in time than the incoming pulse was, which explains the spread of the pulse. To what extent the pulse is spread out in space depends on the adjustment time of the system, which is directly related to the flow velocity through the channel.

The sensitivity to the river width

Figures 4.8, 4.9 and 4.10 show the evolution of river storage, river depth and flow velocity for different values of the river width. The effect of the river width on the flow depth is most straightforward: the flow depth is inversely proportional to the river width ($h = \frac{S}{W \cdot L}$). The effect of the river width on the flow velocity is determined by the wetted

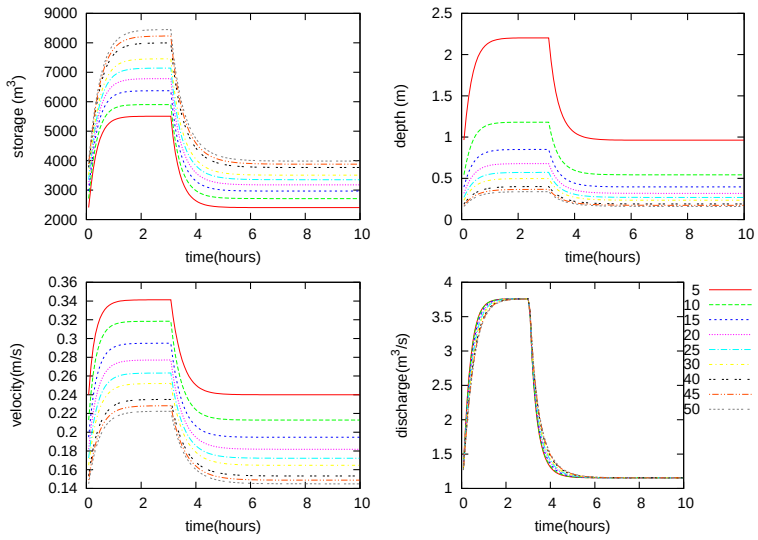

Figure 4.8: *Model output: Evolution of the river storage, flow depth, flow velocity and river discharge for the first grid. Different colors indicate different river widths (ranging from 5m to 50m). At time t=0, a 3 hour during runoff pulse is given of 10 times the spin up value.*

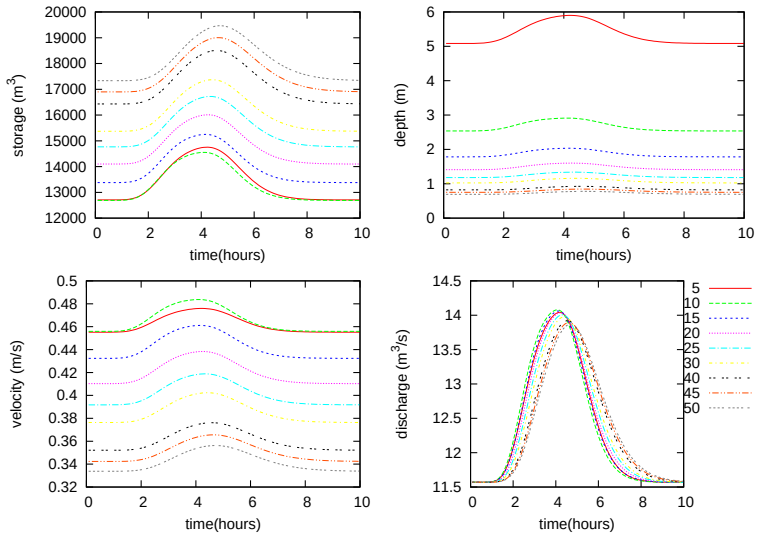

Figure 4.9: *Model output: The same as figure 4.8 but now at a distance of about 5 km from the disturbance.*

perimeter in equation 3.13. For a given storage ($W \cdot h$ is constant), this function has a peak for a certain ratio between the river width and flow depth. The highest values generally occur when channels are deep and narrow (figures 4.8 and 4.9), but when the width is too small the flow velocity is small again (due to friction at the side walls, see figure 4.10). The storage, which in equilibrium is related to the flow velocity by $S = \frac{L}{V} \cdot I$, shows a general increase with increasing river width, but is also high for very small river widths. The sensitivity of the output variables (including the river discharge) to the river width, is largest for very small river widths (smaller than 4 meters or so; 4.10).

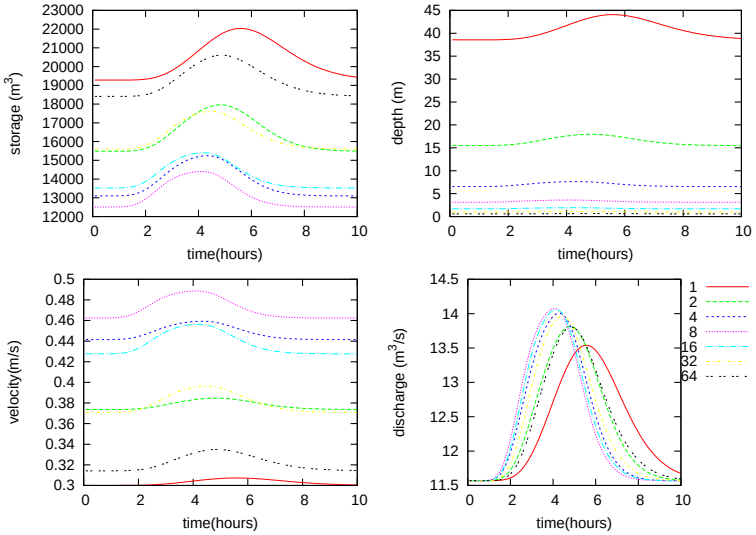

Figure 4.10: *Model output: The same as figure 4.9, but now also for smaller river widths (solid red, dashed green and dashed blue line).*

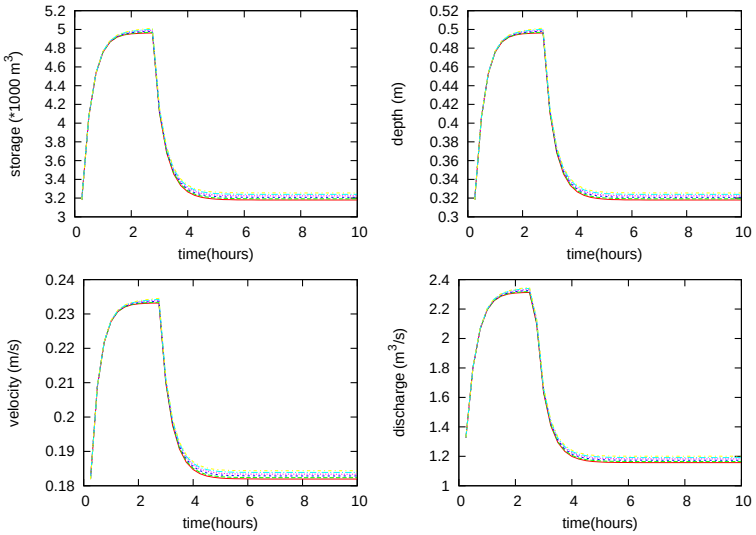

Figure 4.11: *Model output: Evolution of the river storage, flow depth, flow velocity and river discharge after a 2.7 hours long runoff pulse and drainage pulse are supplied simultaneously starting from time zero. Different colors indicate different drainage values, ranging from 1 (solid red line) to 25 (dashed turquoise) times the spin up value. The size of the runoff pulse is five times the spin up value.*

The sensitivity to the groundwater residence time

In figure 4.11, the output variables are plotted for different drainage values. If the effect of a drainage pulse on the output variables is compared with the effect of a surface runoff pulse, it can be concluded that the peak in the output variables as a consequence of the runoff pulse is much larger than the peak in the output variables as a consequence of the drainage pulse. The response of the system to a surface runoff pulse is fast and great, whereas a drainage pulse results in only a small increase in the output variables, but this small increase lasts for a long time. The effect of a drainage pulse on the output variables of a river is much more extended.

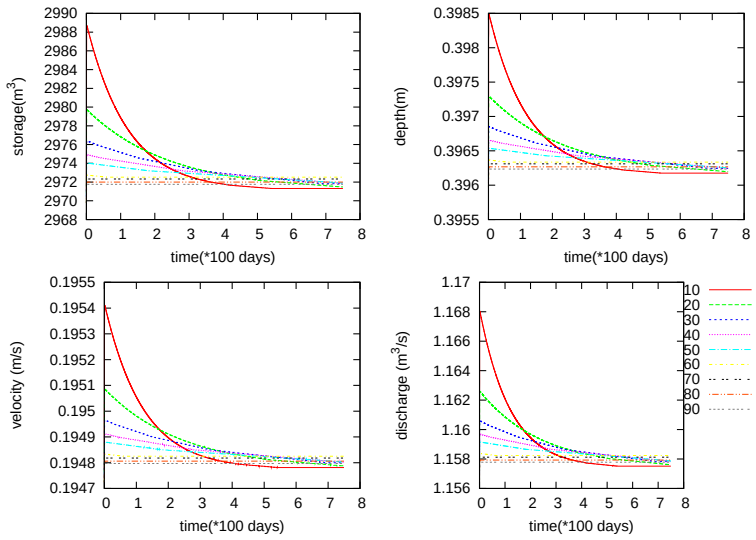

Figure 4.12: *Model output: Evolution of the river storage, flow depth, flow velocity and river discharge for different residence times (ranging from 10 (red) to 90 (gray)). At time t=0, a 3 hours during drainage pulse is given of 10 times the spin up values. The amount of surface runoff was equal to amount in the spin up (no surface runoff pulse)*

Figure 4.12 shows the evolution of river storage, river depth and flow velocity for different values of the residence time in the groundwater reservoirs. The residence time in the groundwater reservoir has the same effect as the flow velocity in the river: it determines the timescale of the adjustment process. It determines on what time scale the drainage is transported from the groundwater reservoir into the surface reservoir. How larger the residence time, the longer the time it takes before the equilibrium values of the outflow parameters are re-obtained again. This residence time is much larger than the travel time between the grid cells in the river channel. The total area under the different colored curves in figure 4.12 are equal and do represent the total amount of drainage that was gathered by the system during the pulse.

The reliability of the output variables

To use TRIP for the validation of land surface models, it is convenient that the output variables are directly related to the runoff and that they are not very sensitive to other properties and parameters (including errors) of the system. The sensitivity of, for instance, the river depth (and its response to a runoff pulse) to the river slope is not very convenient if TRIP-simulations of the river depth are used as an indication for the surface runoff (in the validation process) or for making flooding predictions. The discharge is much less influenced by properties of the system and is therefore a more appropriate variable for testing land surface models and for making flood predictions.

The reliability of the TRIP model will depend on the shape of the runoff and drainage forcing curves. If the input to the system (the amount of runoff and drainage) is changing very slowly, the system can keep up with the changes and will be in equilibrium most of the time. In that case, the river discharge is fully determined by the runoff and drainage forcings and is not sensitive to the sensitivity parameters of the system. However, when the input is changing rapidly, so that the system can not keep up with the changes, the river discharge will be more sensitive to properties of the system. So, TRIP is probably more reliable in areas where the forcings (precipitation, radiance and runoff) are changing

slowly. However, river routing is especially needed to monitor high frequency variabilities in the discharge and adds just more (compared with unrouted estimates of the discharge) in areas where the forcings are changing rapidly.

4.3 Summary and Conclusions

To test the behavior of TRIP, a simple river model has been constructed. This model uses the same equations as TRIP to calculate output variables (river storage, flow depth, flow velocity and outflow discharge), but it is one dimensional and consists of only a few points in space. The system was brought into balance with a given amount of runoff and drainage. When a balance was obtained, a runoff and/or a drainage pulse was applied at the root of the river. The response of the system and the transport of a water pulse through the river channel were monitored. To test the sensitivities of the output variables to parameters (properties of the system as river slope and river width), the model has been run for different values of the drainage, river slope, river width and the residence time in the groundwater reservoir. The following conclusions can be drawn:

- A runoff or drainage pulse (of 1 to 10 times the runoff value for which the system is brought into equilibrium) results in a peak in all output variables (i.e. river storage, flow depth, flow velocity and discharge). The sizes of the peaks depend on the size of the runoff/drainage pulse and on properties of the system as the slope of the river channel and the river width. There is a linear relation between the size of the runoff or drainage pulse and the size of the peak in the output variables (figures 4.3 and 4.4).

- When the pulse travels downstream the river, it is spread out in space and time. To what extent the pulse is stretched depends directly on the adjustment time of the system and hence on the flow velocity in the channel. The flow velocity is sensitive to properties of the system as the slope and the width of the river channel.

- Large river slopes result in large flow velocities. The river slope has therefore an important effect on the timing of pulses (at what time the pulse arrives at a given point). Due to its effect on the flow velocity, the river slope also determines to what extent the pulses are stretched when traveling towards the river mouth. Furthermore, the river slope influences the river storage and flow depth in a channel. A large river slope will result in small equilibrium values of the river storage and flow depth. The response of the storage and flow depth to a runoff pulse are smaller and faster for large river slopes.

- The output variables are also sensitive to changes in the river width. The sensitivity of the output variables (including the river discharge) to the river width is largest for very small river widths (smaller than 4 meters or so).

- The equilibrium value of the discharge is not affected by the properties/parameters of the system. When the system is in equilibrium, the outflow discharge from a grid cell is fully determined by (i.e. in balance with) the inflow into a grid cell.

- A time series of the outflow discharge is sensitive to the flow velocity and river slope. An error in the river slope will result in an error in the flow velocity and a shift in the arrival time of a disturbance at a given point.

- The response of the system to a surface runoff pulse is faster than the response to a drainage pulse. Due to variabilities in the runoff, the output variables will be fluctuating a lot on a small time scale. The effect of a drainage pulse is much more

smoothed out; a drainage pulse will result in a small increase in the output variables, but this small increase lasts for a longer time. The total effect of a drainage pulse and a runoff pulse (integrated over a long time) of the same size will be the same and equal to the inflow.

- The residence time in the groundwater reservoir has the same effect as the flow velocity in the river: it determines the timescale of the adjustment process. It therefore determines the timing of pulses and the spread of pulses in space and time.
- The sensitivity of the river depth, the flow velocity and the river storage (and their response to a runoff pulse) to parameters of the system is not very convenient for validating land surface models or for predicting flood events. Uncertainties in the parameters are translated in errors in the output variables. The discharge, that is much less influenced by properties of the system, is probably more appropriate for testing land surface models and for making flood predictions. However, during the adjustment process to changes in the runoff forcings, also the discharge depends on sensitivity parameters.

5

Tuning parameters

In the following chapters, simulations of the 'real' world rivers by the 2 dimensional TRIP scheme are presented. For these simulations the variable Manning's roughness coefficient (equation 3.12), which was originally used by the TRIP scheme, was replaced by a constant value (section 5.1). The roughness coefficient and the groundwater residence time were tuned as a set for each river separately (section 5.2).

5.1 The effect of the variable roughness coefficient

In the original version of TRIP, the Manning's roughness coefficient is given by equation 3.12. It depends on the hydraulic radius, the cross section of the river and the slope of the riverbed. Figure 5.1 shows discharge simulations for the Amazon river, obtained with the variable Manning's coefficient (purple line) and with constant values of Manning's coefficient (green and orange lines).

The results obtained with the time varying Manning's coefficient were not satisfactory. For all rivers that were considered (at the river mouth), the peaks and valleys in the simulated river discharges lagged far behind the peaks and valleys of the observed river discharge (see figure 5.1). Also, the variance of the graphs was too small. Figure 5.1 clearly shows that the timing and variance of the simulations performed with a variable Manning's roughness coefficient are worse than that of simulations obtained by using a constant n of 0.07 (whereas constant values between 0.015 and 0.03 can be found in literature). This indicates that the use of a time-varying Manning's coefficient causes too much delay of the water. The use of a constant value between 0.01 and 0.03 for the Manning's roughness coefficient considerably improved the variance of the graphs and the coincidences between the valleys and peaks of the simulations with those of the observations. Therefore, a constant Manning's coefficient was further used for the validation process. This constant was tuned for each river separately (section 5.2). Figure 5.2 shows the time series of the variable Manning's roughness coefficient as used for the discharge simulations of figure 5.1.

5.2 Optimizing the delaying parameters in TRIP

The effect of the groundwater residence time (τ_g) and Manning's roughness coefficient are comparable and hard to distinguish. Therefore these parameters where tuned as a set. Simulations with different constant values for the Manning's coefficient (varied between 0.01 and 0.03) and the groundwater residence time (varied between 10 and 80 days) were performed. For each river, the averaged (absolute) time period between the occurrence of the simulated and observed peaks was calculated for all different performances (the coincidences of the valleys were not considered, since the discharge in dry periods is probably more influenced by the infiltration process within the LSM and is therefore

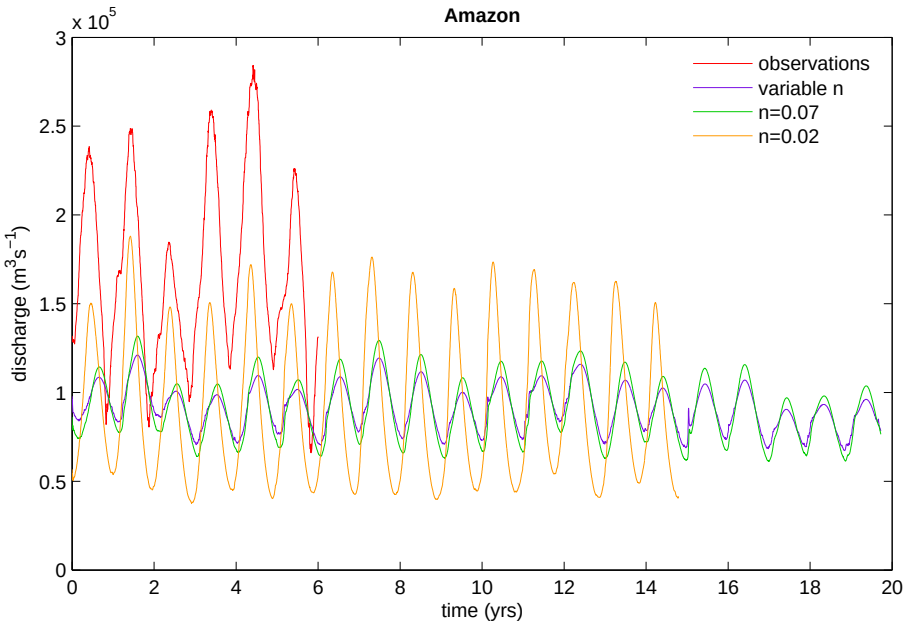

Figure 5.1: *Time series of observed and simulated river discharge at the mouth of the Amazon river. The ticks are placed at the first of January of the indicated year. Runoff values were performed from the online configured* HTESSEL *scheme, coupled with climate model EC-Earth. Observed data is obtained from the Global Runoff Data Center (*GRDC*) for the period 1990-1996. The climate model is initiated with atmospheric data of 1990, but is not further forced with observations. The precise course of the curves can, therefore, not be compared. However, it makes sense to compare statistical quantities as the standard deviation. The standard deviation (for the red, green, purple and orange graphs respectively* $5.1 \cdot 10^4 m^3 s^{-1}$, $1.2 \cdot 10^4 m^3 s^{-1}$, $1.7 \cdot 10^4 m^3 s^{-1}$ *and* $4.2 \cdot 10^4 m^3 s^{-1}$*) of the simulated curves are smaller than the observed standard deviation. Simulations performed with a constant Manning's coefficient of n=0.02 (*τ_g*=50) gives better results than simulations performed with a time-varying Manning's coefficient (*τ_g*=50).*

more sensitive to errors within the LSMs). The performance was selected which coincides best with the simulated and observed discharge peaks. Sometimes the erratic time series of the discharge observations was smoothed a bit (over about 40 days) to determine the exact moment of peaking in a more objective way. This smoothing process did not significantly change the moment of peaking. Examples of analyzed time series are indicated in figure 5.3. For the Amazon river, best coincidences of the peaks were found for a groundwater residence time of 50 days and a Manning's roughness coefficient of 0.01 (for both LSMs). For the Danube river, best coincidences of the peaks were found for a groundwater residence time of 10 days and a Manning's roughness coefficient of 0.01 (for both LSMs).

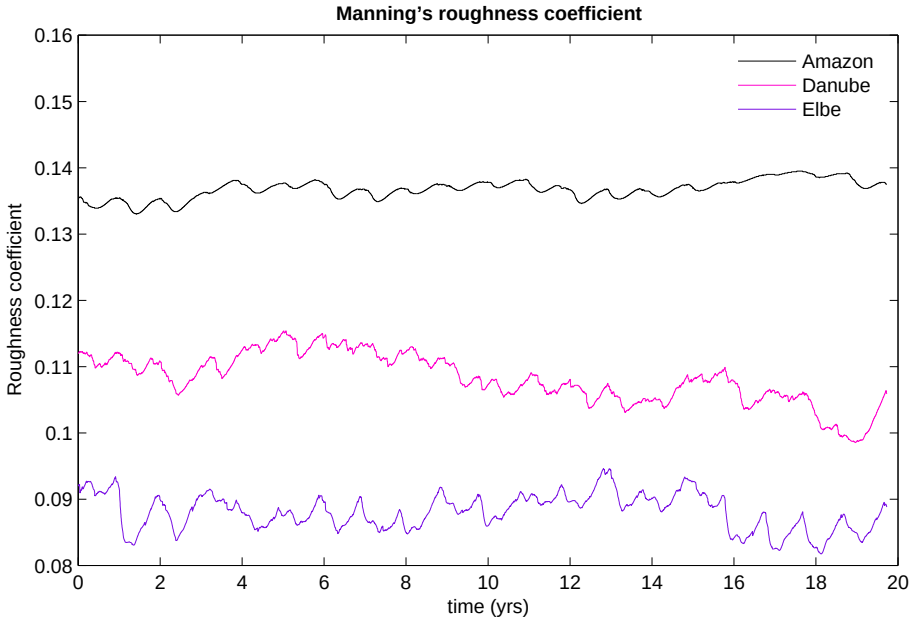

Figure 5.2: *Values of the time varying Manning's roughness coefficient at the river mouths of the Amazon, Danube and the Elbe river during discharge simulations (the values for the Amazon are the values that were used for the discharge simulations in figure 5.1).*

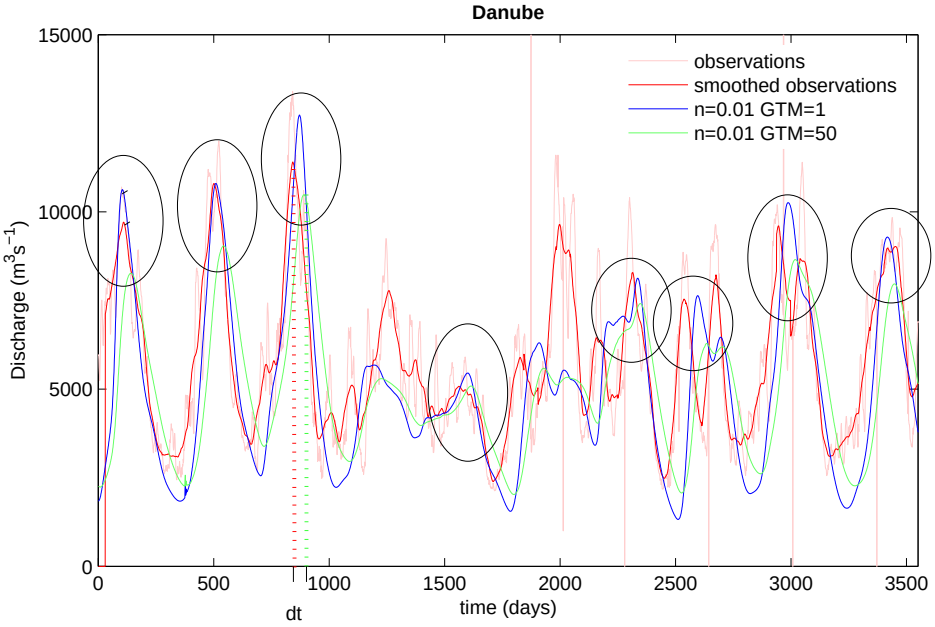

Figure 5.3: *Plot of the time series of the (smoothed) discharge observations and simulations by two different performances of the* TESSEL-TRIP *combination. The parameters in* TRIP *were tuned by considering the coincidences of the simulated and observed peaks. The peaks that were considered in case of the Danube are indicated with ellipses. The best performance was selected on the basis of a minimal time period between the occurrences of the simulated and observed peaks.*

6

River routing for the simulation of real world rivers

A river routing model translates runoff into measurable river discharge. The modeled runoff is thus altered by the river routing model as to be able to compare the runoff with observations.

In this chapter, the way in which TRIP alters the runoff is studied further by comparing unrouted runoff with discharge simulations for the Amazon and the Danube river. Therefore, daily values of the unrouted runoff were integrated over the drainage areas of the rivers. The integrated unrouted runoff can be considered to be a rough estimate of the river discharge, in which the delay of the subsurface runoff in entering the river stream and the travel time of water in the river channel is simply ignored. Discharge simulations were performed with the TRIP model in which the variable Manning's roughness coefficient was replaced by a constant value (the values of the Manning's roughness coefficient and the groundwater residence time were tuned as a set for each river, as explained in chapter 5) and which was forced with daily runoff modeled with the offline TESSEL and HTESSEL land surface models.

6.1 Averaging time and spatial scales

The difference between the discharge that passes the river mouth during a period of time and the amount of unrouted runoff that is created in the total drainage area during that same time period becomes smaller for larger averaging times. Namely, when the averaging time scale is much larger than the travel time of the water through the river channel and also much larger than the groundwater residence time, by far most of the runoff that was created within the long averaging period has reached the river mouth within that period, irrespective of the specific pathway or flow velocity of the water.

However, when one considers the river discharge at smaller time scales, the averaged discharge at the river mouth does depend on the specific pathway and the flow velocity of the water. A similar argument holds for the spatial scale of the drainage basins; the effect of TRIP is large for drainage areas that are of such large size so that the travel time of water through the river is larger than the time over which averages are calculated (figure 6.1). River routing is thus especially needed when one wants to monitor the small temporal scale (daily-monthly) variability of large rivers. For averaging times smaller than about one year, TRIP has a considerable large effect (up to 60% of the total routed discharge) on the estimates of the river discharge in the Amazon and Danube (see figure 6.2).

6.2 The effect of TRIP

The effect of TRIP on the time series, long term averages, variances, cumulative probability plots and frequency spectra of the modeled discharge is investigated in this section. Therefore, the unrouted runoff and the routed discharge are constantly compared.

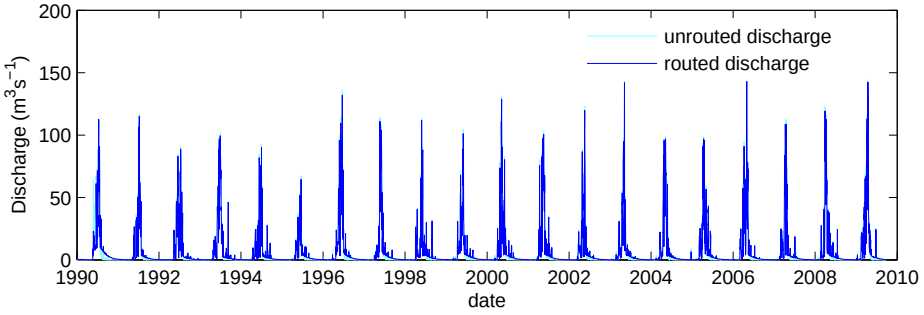

Figure 6.1: *Routed and unrouted discharge simulations for a small river basin. The coupled combination of* HTESSEL *and* EC-EARTH *was used to obtain surface runoff and drainage. The ticks are placed at the first of January of the indicated year. The figure shows that the differences between routed and unrouted runoff are small for small river basins.*

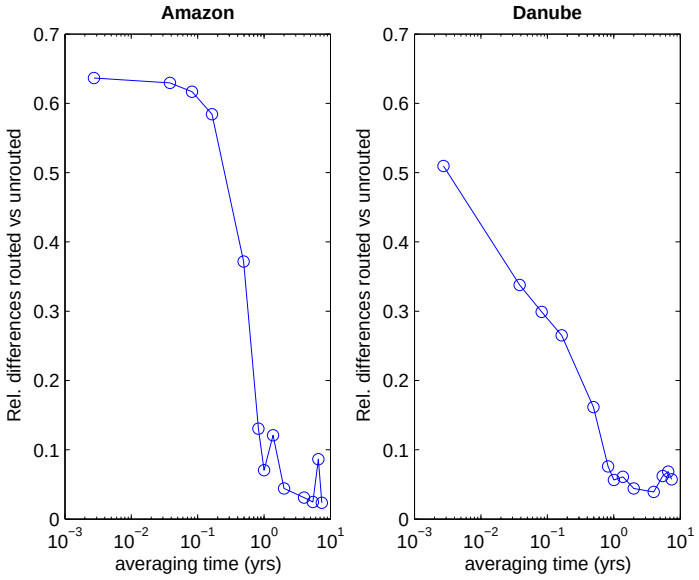

Figure 6.2: *The relative difference between moving averages of the routed and the unrouted discharge are plotted against averaging time. This plot is obtained by taking moving averages (over the indicated averaging time) of the routed and unrouted time series, then taking daily absolute differences (between the smoothed unrouted and smoothed routed time series) and divide these difference by the routed discharge. Finally, the obtained values are averaged over the whole time series. The difference between the routed and unrouted discharge stabilizes at about 5% for long averaging times, which is explained by the spin up criterion that was used by the* TRIP *model (the spin up was ended when the state variables at the end of two successive spin up years was smaller than 5%; section 3.1).*

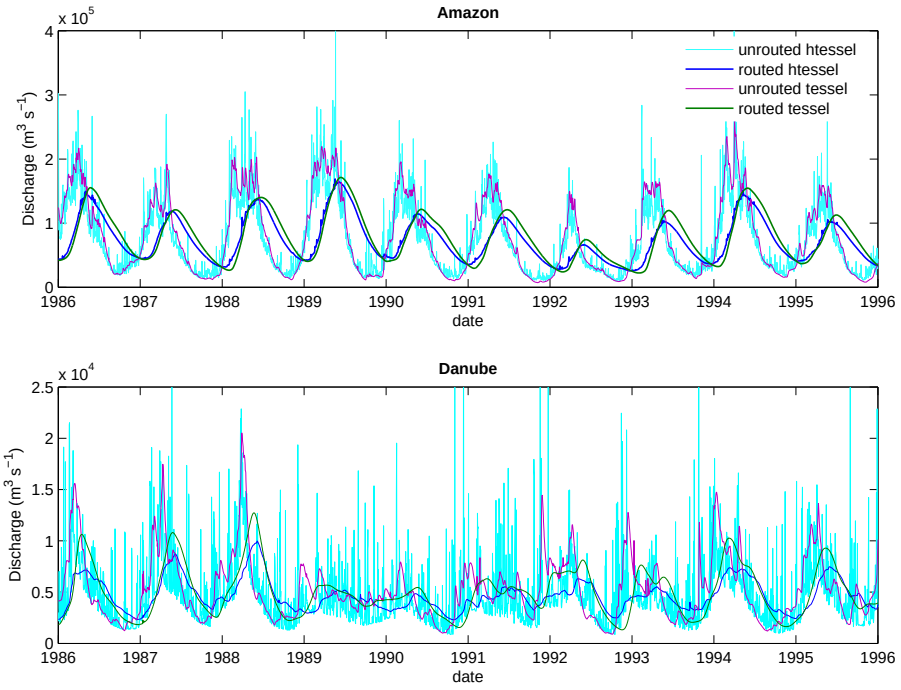

Figure 6.3: *Simulated time series of discharge at the river mouth of the Amazon (upper panel) and for the Danube (lower panel) river. Discharges are estimated with (routed) and without (unrouted) using the river routing model* TRIP. *The input for the* TRIP *scheme (that is runoff and drainage values) was obtained from offline configurations of the* TESSEL *and* HTESSEL *land surface schemes, forced by atmospheric data (the GSWP-2 data set). The ticks are placed at the first of January of the indicated year. Optimized values for the groundwater residence time (50 days for the Amazon and 10 days for the Danube) and the Manning's roughness coefficient (0.01 for both rivers) were used (see section 5).*

The time series

Time series of routed and unrouted simulations of the river discharge of the Amazon and Danube are plotted in figure 6.3. This figure shows that river routing has a delaying effect. For instance in the Amazon river, the simulated discharge peaks in March/April without river routing, shifting towards May/June when river routing is applied. Also in the Danube river the delaying effect of river routing is clearly visible. Figure 6.3 furthermore shows that river routing also results in smoother graphs and less variability at a small spatial scale. In chapter 4, it was already noted that peaks and valleys in the river discharge are spread out in space and time while the water is traveling downstream the river. To what extent the smoothness and the variability of the graphs is altered depends on the residence time of the groundwater and the flow velocity through the channel and is directly related to the delay of the water traveling down through the river.

The long term average

In essence, river routing should only delay water and should not affect the long term averaged runoff. The 10-years-averaged routed and unrouted simulated discharge (figure 6.3) are for the TESSEL simulations of the Amazon both (routed and unrouted) $7.8 \cdot 10^4 m^3 s^{-1}$ and for the HTESSEL simulations both $7.4 \cdot 10^4 m^3 s^{-1}$. For the Danube, the 10-years-averaged routed and unrouted runoff differ slightly. For the TESSEL simulations routed and un-

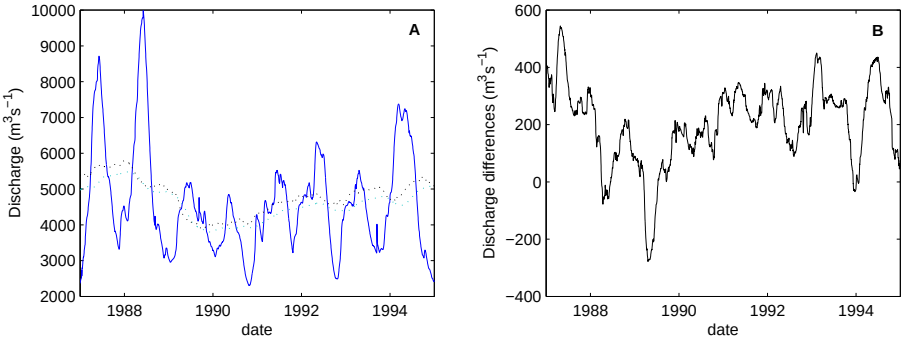

Figure 6.4: *A: Plots of the simulated discharge (dark blue line) and the two-years-moving-averages of the routed discharge (dotted light blue line) and unrouted runoff (dotted black line). The underestimation of the long term average by* TRIP *is small (5%) compared with the yearly variability in the discharge. B: Differences between the two-years-moving-averages of the routed discharge and unrouted runoff. Although the difference in the long term average is probably explained by a limited spin up in* TRIP*, it does not clearly decrease during this 10 years period.*

Table 6.1: *Standard deviations Amazon*

	TESSEL	HTESSEL
routed	$3.7 \cdot 10^4 m^3 s^{-1}$	$3.4 \cdot 10^4 m^3 s^{-1}$
unrouted	$6 \cdot 10^4 m^3 s^{-1}$	$5.6 \cdot 10^4 m^3 s^{-1}$

Table 6.2: *Standard deviations Danube*

	TESSEL	HTESSEL
routed	$2.4 \cdot 10^3 m^3 s^{-1}$	$1.5 \cdot 10^3 m^3 s^{-1}$
unrouted	$3.2 \cdot 10^3 m^3 s^{-1}$	$3.4 \cdot 10^4 m^3 s^{-1}$

routed averages are $5.0 \cdot 10^3 m^3 s^{-1}$ and $5.3 \cdot 10^3 m^3 s^{-1}$ respectively (a difference of 6%) and for the HTESSEL simulations $4.7 \cdot 10^3 m^3 s^{-1}$ and $4.9 \cdot 10^3 m^3 s^{-1}$ respectively (a difference of 4%). These small differences in the long term averages of the routed and unrouted runoff are probably explained by the criterion that was used for the spin up in TRIP: the spin up has been ended when the differences between the state variables at the end of two successive spin up years was smaller than 5% (see section 3.1). Therefore, the rivers in TRIP might not have been entirely in balance with the typical yearly runoff forcings. In figure 6.4, the two-years-moving averages over both the routed and unrouted HTESSEL runoff are plotted together with the HTESSEL-TRIP modeled discharge. The figure shows that the difference between the two years averages of the routed and unrouted runoff are about 5% of the yearly variability in the routed discharge. Furthermore, these differences do not show a clear decrease over the plotted time period (i.e. the period over which two-years-moving-averages could be calculated). Since the overall underestimation by the TRIP model (due to the limited spin up that was applied) is small compared with the typical variabilities in the discharge, it is assumed that its effect on the (variabilities in the) simulations is limited (approximately 5-10%).

The standard deviations

River routing alters the variance of the runoff. The standard deviations of the daily simulated runoff and discharge from the 10 years average are indicated in table 6.1 for the

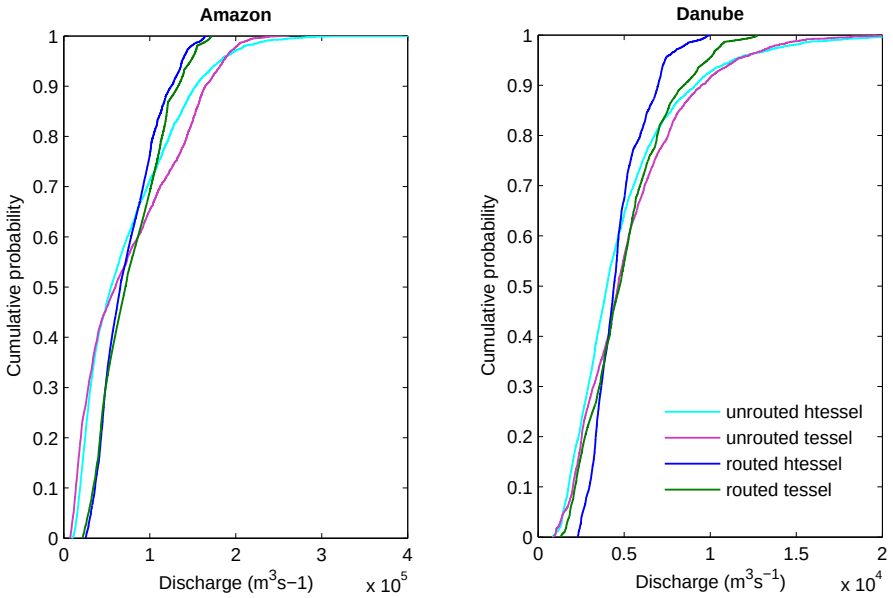

Figure 6.5: *The cumulative probabilities of the data in figure 6.3. In these plots, simulated and observed river discharges of the Amazon and Danube river are plotted on the x-axis and the y-axis indicate the probability of occuring of discharges that are smaller than or equal to the indicated discharge on the x-axis. The routed simulations show steeper curves than the unrouted simulations.*

Amazon and in table 6.2 for the Danube. Note that for the Danube river (where the differences between the TESSEL and HTESSEL discharge is larger than in the Amazon river), the river routing process influences the variance of the HTESSEL simulations much more than the variance of the TESSEL curve. Although the HTESSEL land surface scheme produces much more variability in the runoff than the TESSEL scheme, after river routing the variance of the HTESSEL curve is smaller than that of the TESSEL curve. The different effect of TRIP on the TESSEL and HTESSEL runoff is explained by the different time scales on which the TESSEL and HTESSEL schemes produce variability in the runoff (figure 6.6). The HTESSEL scheme produces much more variability on a time scale of days (due to the creation of surface runoff), whereas the TESSEL scheme produces more variability on a time scale of months (all the water participates in the slow infiltration process). Since TRIP acts on a time scale of weeks to months, the daily variance is averaged out by the TRIP model, whereas the variance on a time scale of months is less affected. The different effects of river routing (and probably the river streams in nature) on (especially the small term variability of) the HTESSEL modeled runoff compared with the TESSEL modeled runoff rise the question whether TRIP suppresses the high frequencies in the HTESSEL runoff too much or whether this is all explained by the nature of the streamflows. Dependent on the answer on this question, the following question should concern the use of TRIP or streamflows (at these large spatial scales) in general for the validation of these land surface models. It might also be that TRIP was not functioning optimally.

The cumulative probabilities

Figure 6.5 shows the cumulative probability distribution of the unrouted runoff and the routed discharge in the Danube and Amazon. The cumulative probability indicates the probability that the discharge (or unrouted runoff) is less than or equal to the specified value on the x-axis. The steeper the probability curve is, the smaller the variability in

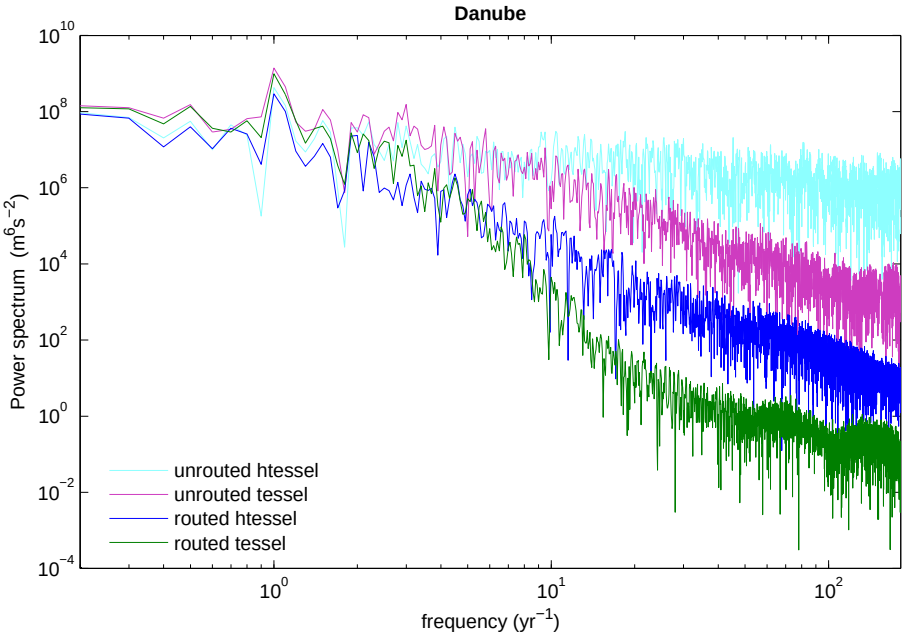

Figure 6.6: *Power spectra of the routed and unrouted runoff simulations for the Danube region. TRIP reduces the contribution of the high frequency components to the variance.*

the discharge. The figure shows that river routing reduces the variability in the river discharge. The extreme values are reduced. The cumulative probabilities for the Danube show again that the effect of river routing on the HTESSEL runoff is much larger than its effect on the TESSEL runoff (the steepness of the HTESSEL curve is altered more). Whereas one might expect that the HTESSEL scheme produces more short term variability and larger extreme values than the TESSEL scheme, the figure shows otherwise.

The frequency spectra

To get insight into the way in which the total variance is distributed over the different frequency components, the frequency spectra is considered. The spectrum indicates for each scale of motion (i.e. each frequency or time period) its relative contribution to the total variance. The spectra in figure 6.6 shows that especially the high frequency components of the variance are filtered out by the TRIP scheme. The figure shows that the contribution of the high frequency components to the total variance is much smaller for the routed as for the unrouted runoff.

6.3 The effect of the delaying parameters in TRIP

The most important function of a river routing model is to delay water, as to approach the delay that drainage and surface runoff experiences in reality in entering river channels and following these rivers towards the river mouth. The delay of the water smoothes the time series of the runoff and reduces its variance.

In TRIP, there are two important parameters which determine the delay of the runoff: the groundwater residence time τ_g determines the delay of the drainage in entering the river streams (equation 3.2) and the Manning's roughness coefficient n influences the flow velocity through the river channel (equation 3.11).

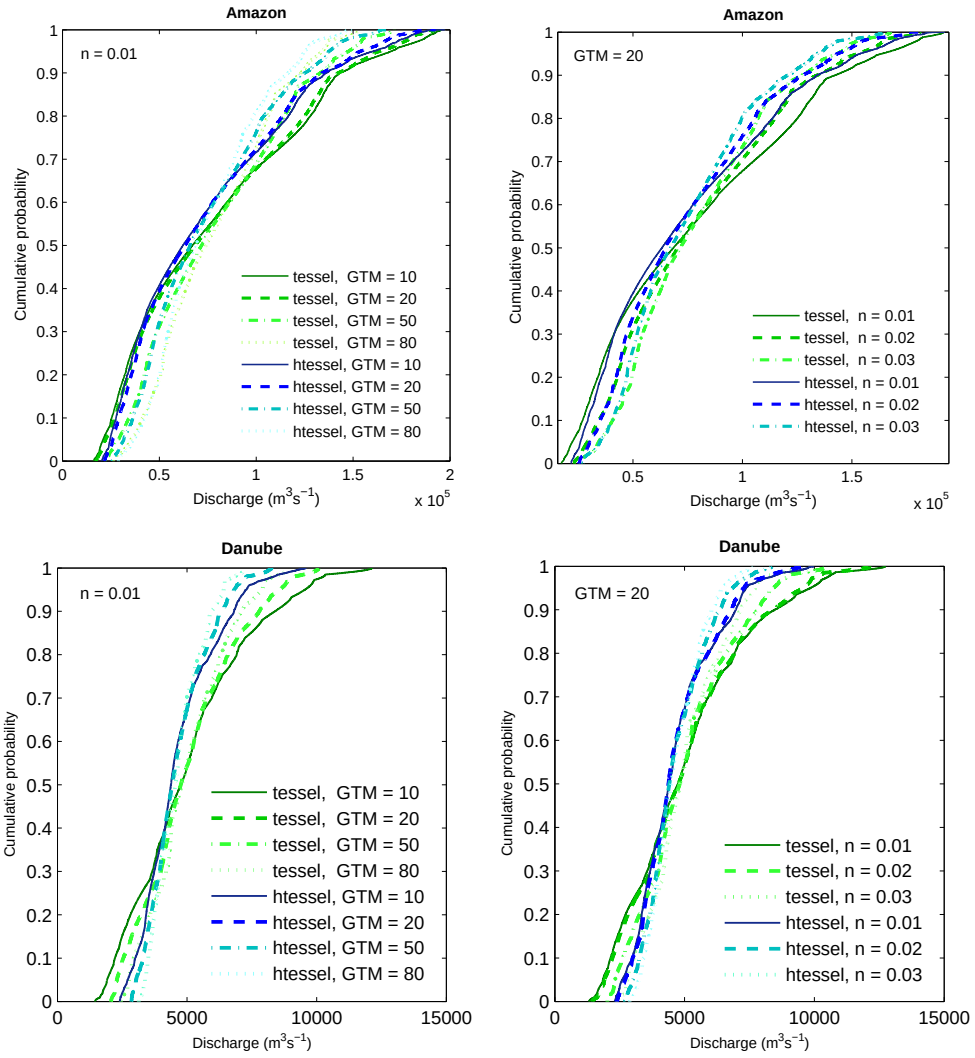

Figure 6.7: *Cumulative probability plots of the discharge at the river mouths of the Amazon (top) and Danube (bottom) rivers, derived with different values of the ground residence time and Manning's roughness coefficient in the* TRIP *routing scheme. Runoff was obtained from the* TESSEL *and* HTESSEL *schemes, both forced with atmospheric observations.*

To get more insight in the effect of the delaying parameters in TRIP (and of the errors within these parameters), the groundwater residence time and the Manning's roughness coefficient were varied to obtain different discharge simulations. The Manning's roughness coefficient and the groundwater residence time were varied between $n = 0.01$ and $n = 0.03$ (this are values that can be found in literature for the major rivers on Earth (Lucas-Picher et al, 2002)[12]) and between 10 and 80 days respectively. A simulation that was performed with a specific combination of a LSM, a groundwater residence time and a roughness coefficient is hereafter called a specific *performance*.

In figure 6.7, the cumulative probabilities of the river discharge are plotted for the different performances. The figure shows that the steepness of the cumulative probability curve increases with increasing roughness coefficients and with increasing groundwater residence times and hence, with increasing time delay. This is in agreement with the effects of TRIP on the unrouted runoff as discussed in section 6.2.

For a comparison between the TESSEL and HTESSEL schemes, it would be convenient that the effect of using different parameters in TRIP on the discharge simulations is smaller than the effect of using the HTESSEL land scheme instead of the TESSEL land scheme. In case of the Danube river, the two areas that are set up by the cumulative probability curves of simulations performed with the same land surface model, but with different parameters in TRIP (the lower panels in figure 6.7), barely overlap each other (the blue curves lay separate from the green curves). This means that the models are mutually very different. In other words, the answer to the question *Which land surface model behaves better?* does not depend on the delaying parameters in TRIP. This makes the validation process easier when the observations are located within one of the two colored areas.

For the Amazon, the areas set up by the green and blue lines overlap each other a lot. This means that it is often impossible to say, with some certainty, which LSM is better in agreement with the observations, since a small error in TRIP can lead to another conclusion.

6.4 Conclusions

Conclusions of this chapter are:

- River routing has a delaying effect. This results in a time shift in the time series of the river discharge compared with the time series of the integrated unrouted runoff. The delay of the water smoothes the time series of the discharge estimates and it reduces its variance and high frequency variability. The effect of TRIP on the long term averaged discharge (larger than about 1 year for major rivers) is small.

- The HTESSEL runoff is affected differently by the TRIP scheme than the TESSEL runoff in the way that especially the high frequency variabilities are damped by the TRIP model. This is not very convenient for the validation process. The question has been risen whether TRIP suppresses the high frequencies in the HTESSEL runoff too much or whether the damping of the high frequencies should fully be ascribed to the nature of the streamflows. More insight can be obtained when discharge observations are considered (chapter 7).

- By comparing river discharges calculated by the TESSEL-TRIP and HTESSEL-TRIP combination, no judgment can be pronounced on which scheme (TESSEL or HTESSEL) behaves better in the Amazon region, since the differences between the river discharges are too small in this region. Errors in the TRIP scheme might have large effect on the conclusion.

7

Offline validation

In this chapter, routed and unrouted estimates of the discharge in the Amazon and Danube are compared with observations. If discharge simulations are not improved by river routing, this indicates large errors in the LSMs or TRIP scheme. The question addressed in this chapter is: *Which errors in the river discharge simulations can be explained by the river routing process and which errors should be ascribed to the* LSMs*?* Only discharge simulations obtained from the offline TESSEL and HTESSEL schemes (in combination with TRIP) are considered in this chapter (the online validation is presented in chapter 8). The routed simulations were obtained by using the tuned values of the Manning's coefficient and the groundwater residence time (chapter 5.2). Sometimes, also different performances (using different values of the delaying parameters) are studied.

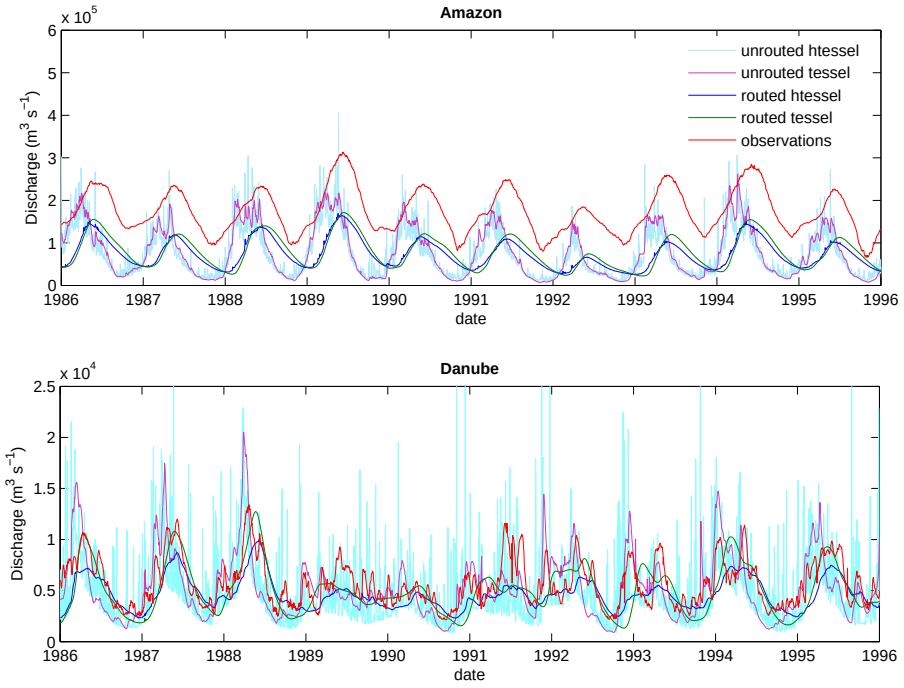

Figure 7.1: *As figure 6.3, but now also the observed river discharge is plotted (red line).*

Table 7.1: *Absolute errors Amazon*

	TESSEL	HTESSEL
routed	$2.0 \cdot 10^4 m^3 s^{-1}$	$1.7 \cdot 10^4 m^3 s^{-1}$
unrouted	$3.0 \cdot 10^4 m^3 s^{-1}$	$3.1 \cdot 10^4 m^3 s^{-1}$

7.1 The time series

Figure 7.1 shows that the TRIP scheme improves the timing of the peaks in the discharge simulations. The moments of low water, however, are not improved by the river routing process, which can best be seen in the Amazon. The valleys in the discharge (i.e. the routed runoff curves) are here lagging behind the observations (this was obtained for all tested performances). This rises the question whether this error (in the form of a delay) should be ascribed to the river routing process or to the LSMs. An explanation that relates the time lag of the valleys to TRIP is that the groundwater residence time is too large. A possible explanation that relates the time lag of the valleys to the LSMs is that the modeled infiltration process is too slow or that the vertical layers in the land surface models are too deep. Especially in dry periods this will lead to errors (in the form of too much delay); the soil is then unsaturated and, after a rain event, water will infiltrate down to the deepest soil. In wet periods, on the other hand, the soil is more saturated. After a rain event during a wet period, more water will run off in the upper layers, which leads to a faster response of the runoff to rain events (i.e. in wet periods, the water does not experience the total depth of the soil). In case of a too slow infiltration process or too deep soil layers, the routed runoff will thus lag the observations in dry periods, whereas it might agree with the observations in wet periods. This is exactly what figure 7.1 shows for the Amazon.

Overall differences

The TESSEL and HTESSEL runoff simulations especially differ at short time scales (see figure 2.7). As to be better able to compare the course of the modeled runoff graphs with observations, the two-years-moving-averages were subtracted from both the simulations and observations (see figures 7.2). Once the two-years-moving-averages were subtracted , the averaged absolute difference between the modeled and observed discharge (also called the absolute error) was calculated. The absolute error is here defined as:

$$s = \frac{\sum_i \sqrt{(Obs_i - Sim_i)^2}}{N}, \tag{7.1}$$

where N is the number of components (that is the number of days) in the time series and i is the index of the components (that is the day-number). The absolute errors for the routed and unrouted TESSEL and HTESSEL runoff in the Amazon and Danube are indicated in tables 7.1 and 7.2. The values in these tables indicate that, when the long-term averages are subtracted from all time series, river routing reduces the absolute difference between observations and simulations. Furthermore, the absolute errors in the HTESSEL-TRIP simulations are smaller than the absolute errors in the TESSEL-TRIP simulations for both rivers.

7.2 The long term average

Perhaps the most striking feature of the simulations for the Amazon river (the upper panel of figure 7.1), is the overall underestimation of the river discharge. The 10-years

Table 7.2: *Absolute errors Danube*

	TESSEL	HTESSEL
routed	$1.4 \cdot 10^3 m^3 s^{-1}$	$1.1 \cdot 10^3 m^3 s^{-1}$
unrouted	$1.5 \cdot 10^3 m^3 s^{-1}$	$1.8 \cdot 10^3 m^3 s^{-1}$

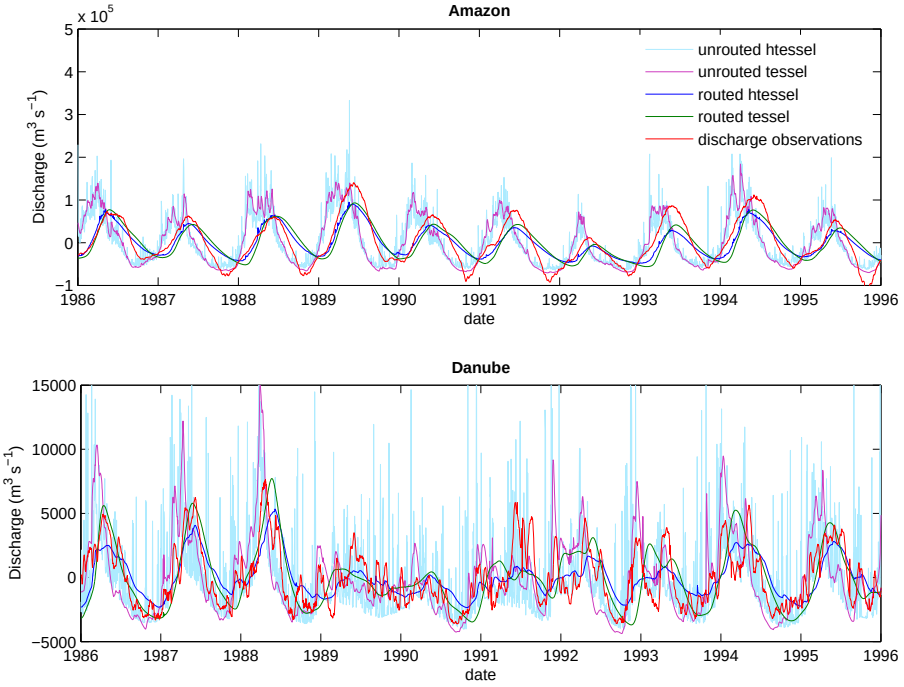

Figure 7.2: *As figure 7.1, but now 2-years moving averages are subtracted from the time series.*

average of the modeled discharge is only about 45% of the observations. This overall underestimation is the same for the routed as for the unrouted discharge and can thus not be ascribed to the river routing process. Although the precipitation measurements and the discharge data from the Global Runoff Data Centre (GRDC) do also contain errors (which are estimated to be 10%-30%), the most likely explanation for the lack of runoff is an overestimation of the evaporation by the LSMS. This explanation is supported by the small modeled runoff fractions in the Amazon. Averages of the modeled and observed runoff fractions were determined by dividing respectively the averaged modeled runoff and the averaged observed discharge by the averaged observed precipitation and were found to be 0.19 (HTESSEL) and 0.21 (TESSEL) versus an observed averaged runoff fraction of 0.46.

For the Danube, there is also a small overall underestimation of the runoff. For the Danube the averaged runoff fractions are: 0.27 (HTESSEL), 0.30 (TESSEL) and 0.32 (observed).

7.3 The standard deviations

Standard deviations (of the daily data from the 10-years average) of the discharge simulations and observations are given in table 7.3. The table shows that the variance in the

Table 7.3: *Standard deviations*

	Amazon	Danube
routed TESSEL	$3.7 \cdot 10^4 m^3 s^{-1}$	$2.4 \cdot 10^3 m^3 s^{-1}$
routed HTESSEL	$3.4 \cdot 10^4 m^3 s^{-1}$	$1.5 \cdot 10^3 m^3 s^{-1}$
unrouted TESSEL	$6 \cdot 10^4 m^3 s^{-1}$	$3.2 \cdot 10^3 m^3 s^{-1}$
unrouted HTESSEL	$5.6 \cdot 10^4 m^3 s^{-1}$	$3.4 \cdot 10^4 m^3 s^{-1}$
GRDC-data	$5.1 \cdot 10^4 m^3 s^{-1}$	$2.6 \cdot 10^3 m^3 s^{-1}$

discharge are underestimated by the simulations. The river routing process only improves the variance in the simulated discharge for the TESSEL runoff simulations in the Danube. Because the variances in the modeled (unrouted) runoff are much larger (also larger than the observations), the underestimation of the routed discharge might perhaps partly be ascribed to the TRIP model. Especially the effect of TRIP on the HTESSEL runoff was found to be large, as explained in chapter 6.

7.4 The cumulative probabilities

In figure 7.3, cumulative probabilities of the modeled and observed discharge in the Amazon and Danube are plotted for different values of the groundwater residence time and Manning's roughness coefficient in the TRIP routing scheme. This figure shows that, for both rivers, the steepness of the cumulative probability curves is best in agreement with the observations when relatively small delaying parameters are used in TRIP.

In the Amazon, the slope of the cumulative probability plot for the 10% smallest discharges can not be obtained by the TRIP model (for all performances). This feature should be ascribed to the land surface models since even the smallest values of the raw unrouted runoff show less deviation from the norm than the smallest observed discharges. Possible explanations are that the slope in this region is influenced by the overall underestimation of the runoff (due to an overestimation of the evaporation) or that the extreme low runoff values calculated by the LSMs are not small enough. The infiltration process might be too slow or the soil layers too deep.

The steepness of the HTESSEL curves for the Danube indicates that the water is too much delayed in the Danube by the HTESSEL-TRIP combination (for all tested parameters).

7.5 The frequency spectra

The variance in the routed runoff simulations were underestimated by both LSM-TRIP combinations for both rivers. The power spectrum of the observed discharge in the Amazon (figure 7.4), shows that the contribution to the variance of frequencies larger than a few times per year is very small in the Amazon. The variance in the discharge data is especially determined by larger scale variabilities. This can also be seen in figure 7.5, which indicates that only about 10% of the variability is contributed by variabilities with frequencies up to once every half year. The observed small contribution of high frequency variabilities to the variance is better represented by the routed than by the unrouted runoff. Since the TESSEL and HTESSEL runoff especially differ at small time scales, the damped high frequency variabilities in the Amazon also explain the small differences between the TESSEL-TRIP and HTESSEL-TRIP discharge simulations. The remaining differences in the discharge is too small to pronounce judgment on which scheme behaves better in the Amazon region.

In section 7.3 and 7.4 it was found that the modeled discharge in the Danube is smoothed too much. This is also confirmed by the power spectra in figure 7.6, which

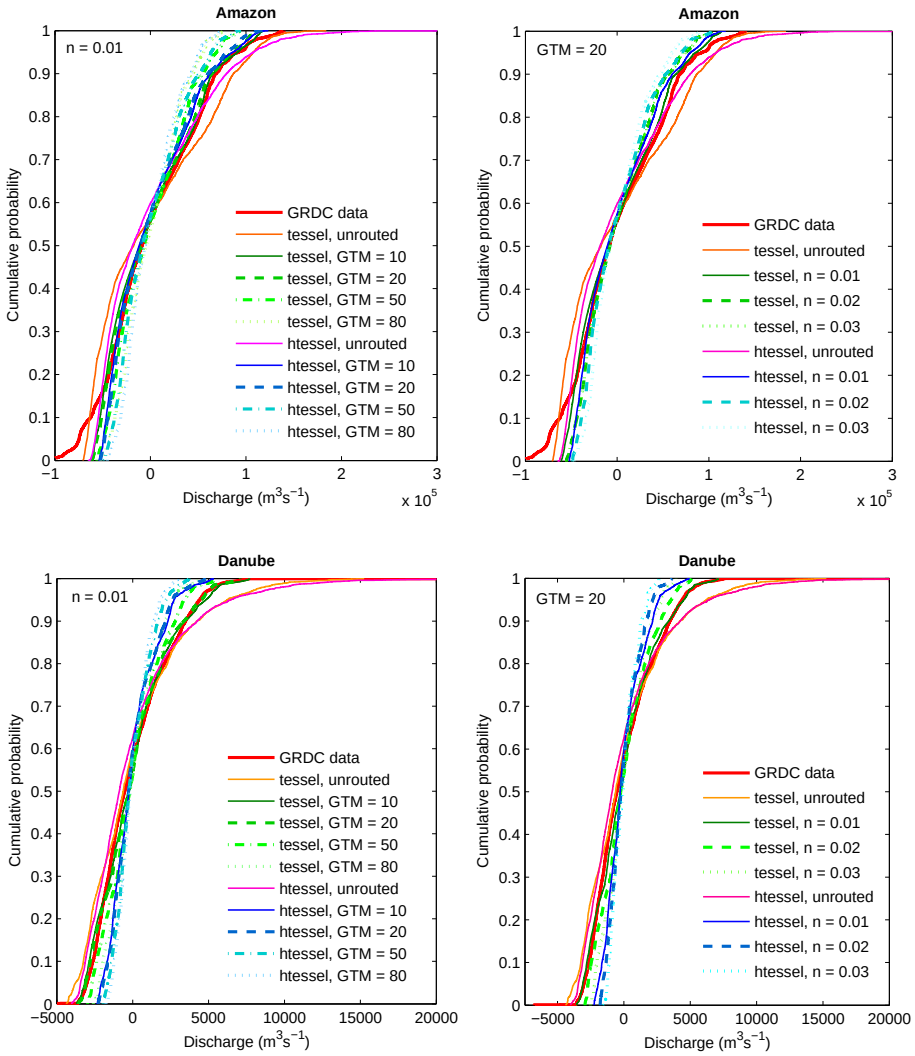

Figure 7.3: *Cumulative probability plots of the discharge at the river mouths of the Amazon (top) and Danube (bottom) rivers, derived with different values of the ground residence time and Manning's routhness coefficient in the* TRIP *routing scheme. The cumulative probabilities of the unrouted simulations and observations are also plotted. The 10-year-average was subtracted for all time series, as to compare the steepness of the curves.*

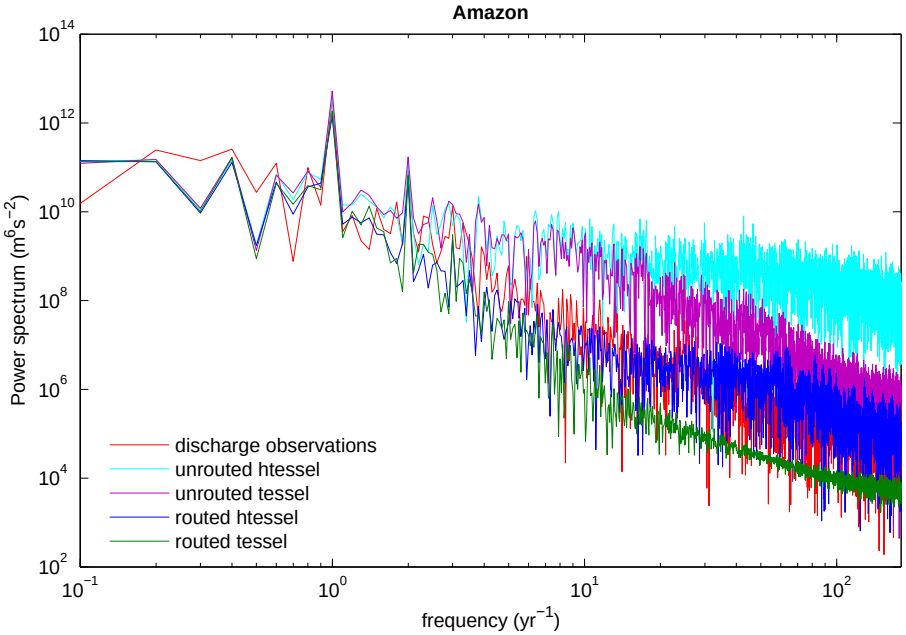

Figure 7.4: *Power spectrum of the routed and unrouted runoff simulations and of the discharge observations in the Amazon.*

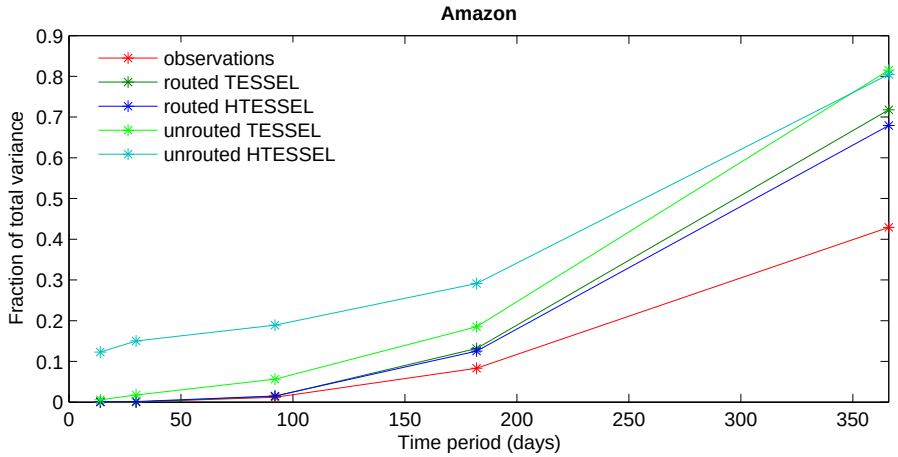

Figure 7.5: *The fraction of the total variance with specific time scales of up to two weeks, one month, three months, half a year and a year for unrouted* HTESSEL *(light blue), unrouted* TESSEL *(light green), routed* HTESSEL *(dark blue), routed* TESSEL *(dark green)and the* GRDC *data (red) in the Amazon river*

.

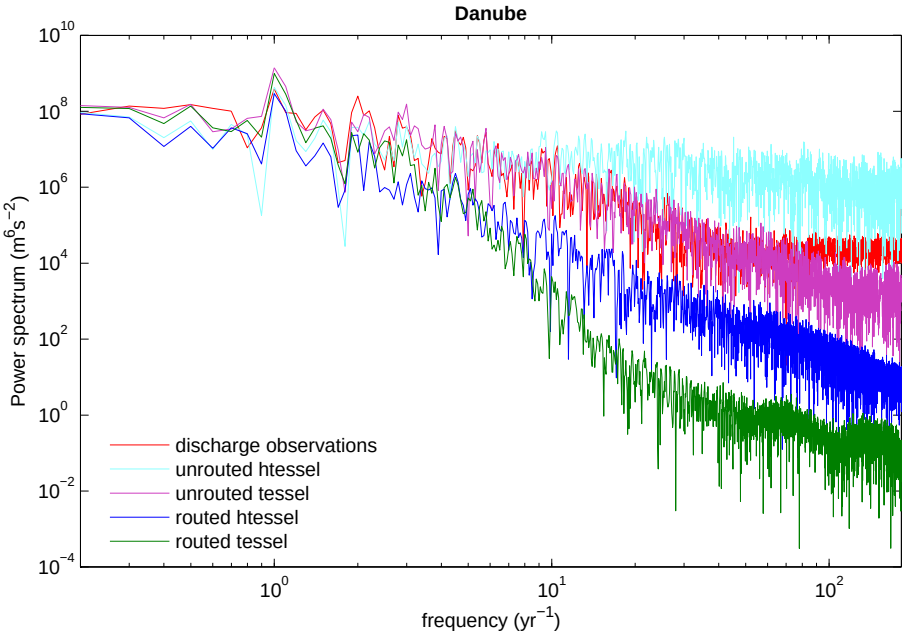

Figure 7.6: *Power spectrum of the routed and unrouted runoff simulations and of the discharge observations in the Danube. The figure shows that the routed simulations have a lack of high frequency components. For the* HTESSEL *simulations this is most likely a effect of river routing, since the unrouted* HTESSEL *runoff does contain much high frequency variability.*

shows a lack of high frequency varibiability for both LSM-TRIP combinations. For the TESSEL-TRIP system, the surplus of smoothing can (partly) be explained by the LSM: the power spectrum of the unrouted TESSEL runoff already shows a lack of high frequency components. For the HTESSEL-TRIP combination it is most likely that the TRIP scheme is damping the high-frequency components in the HTESSEL runoff too much, since the unrouted HTESSEL runoff contains much high frequency variability. This rises the question whether TRIP has the general tendency to damp the high frequency variabilities too much or whether the TRIP was not functioning optimal here (for example the spin up criterion that was used (of 5%) might have been too weak).

7.6 A simple translation method

The results presented in the previous sections suggest that there is too much delay of the discharge simulations. In the Amazon, the extra delay is especially visible in periods of low water, and is probably related to the delay in the drainage. In the Danube, the contribution of high frequency components to the variance is underrepresented. In both cases, the extra delay results in an underestimation of the variance. These features might be due to errors in the TRIP scheme.

To compare the TRIP simulations with otherwise obtained estimates of the discharge, an other, but very simple, approach has been found to translate runoff into river discharge. An attempt is made to estimate the river discharge from the unrouted runoff by shifting the unrouted runoff in time and by taking a moving average over a certain time period (note that a time shift and smoothing of the data were the most important effects of river routing; chapter 6). In fact, for this approach, the runoff has been spread out over a certain time period which follows after the moment of runoff formation (see figure 7.7).

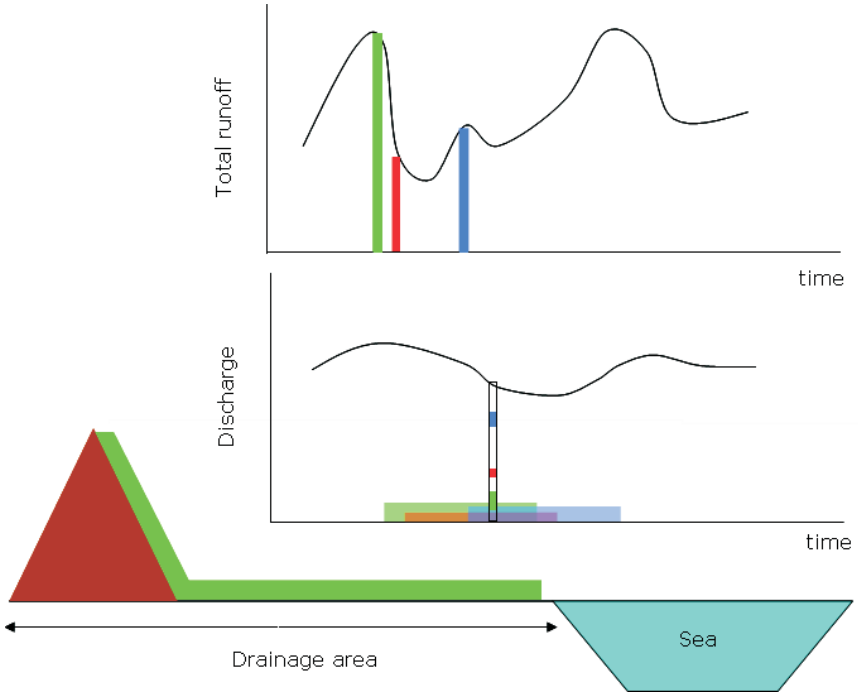

Figure 7.7: *Rough estimates of the river discharge can be obtained by spreading the total unrouted runoff out over a certain time period after its formation, which accounts for the differences in the travel time due to the large spatial dimensions of the river basin.*

The physical explanation for this approach is that, since the runoff is not coming from one position (but is spread over the total drainage area), the total runoff that was created at one specific moment in time will be spread out in time when it arrives at the river mouth. The only parameter that was needed (per river basin) to obtain discharge estimates in this way was the specific time period over which the runoff is spread out in time when it reaches the river mouth. This time period depends on the spatial extend of the runoff and hence on the size of the drainage area and can be determined by considering the size of the river basin and by assuming a constant flow velocity of about 0.5 to 1 m/s (the results were not very sensitive to the exact values of the size of the river basin and the constant flow velocity as long as the values were chosen with some sense). For the results that are shown in this thesis, however, the period of smoothing was optimized by considering the typical time lag between the time series of the unrouted runoff and the discharge observations (thus, as the parameters in TRIP, also this parameter was tuned by considering the coincidences of the runoff peaks (rather than by considering statistical quantities as the variance)). The runoff was then smoothed over twice this time period (therefore it was assumed that the runoff is distributed equally over the river basin and hence that the typical lag between the unrouted runoff and the discharge corresponds to the travel time of the runoff that is formed in the middle of the basin).

In the Amazon (figure 7.8), the discharge observations could best be approached by applying a time shift of 60 days forward in time (note that a shift forward in time corresponds to a delay of the water) and smooth the data over 120 days (the length of the Amazon river (about 7062 km) and the travel time of 120 days then indicate a flow velocity of about 0.5 m/s). As for the TRIP simulations, the peaks in the manipulated runoff do better coincide with observations than the valleys. The timing of the valleys in the manipulated unrouted runoff is better in agreement with observations than the timing of

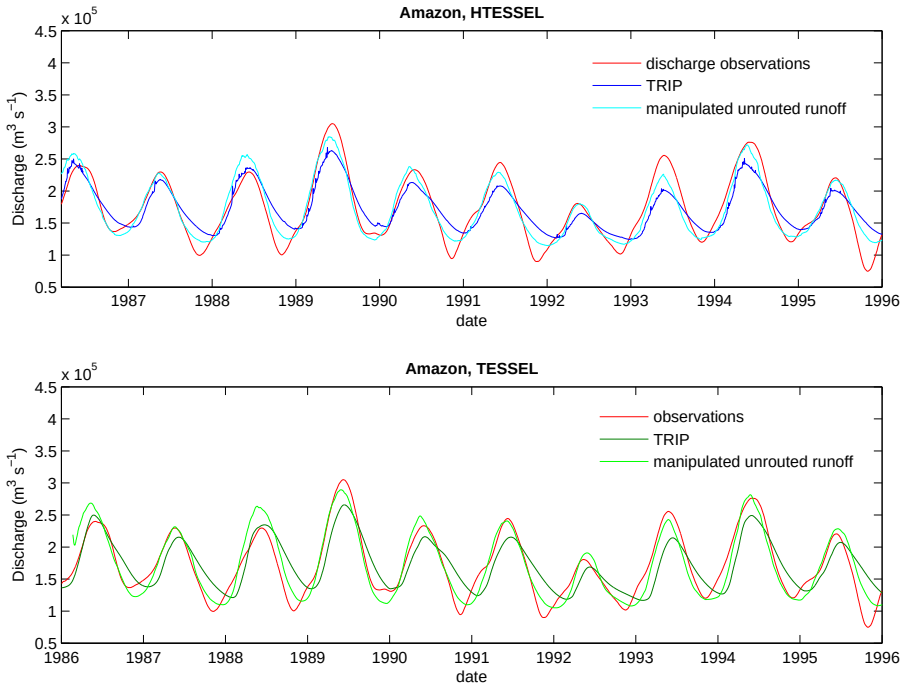

Figure 7.8: *Plots of the discharge observations,* TRIP *simulations and manipulated unrouted runoff for the* HTESSEL *(upper panel) and* TESSEL *(lower panel) scheme in the Amazon. The unrouted discharge was shifted 60 days forward in time and smoothed over 120 days. The modeled discharges were corrected for the underestimation in the 10-years average of the runoff, as to be able to compare the course of the graphs.*

the valleys in the TRIP simulations.

In the Danube (figure 7.9), this simple translation method could improve the HTESSEL discharge estimates (in comparison with the HTESSEL-TRIP discharge) in terms of the standard deviation ($2.1 \cdot 10^4 m^3 s^{-1}$ versus $2.3 \cdot 10^4 m^3 s^{-1}$ for the observations), the cumulative probabilities (see figure 7.11) and the higher frequency end of the power spectrum (figure 7.10). This improvement was obtained by shifting the unrouted runoff over 20 days and by taking moving averages over 40 days (which corresponds to a flow velocity of about 2829 km/40 days=0.8 m/s).

The simple translation method could not improve the variance and the cumulative probabilities of the TESSEL-TRIP discharge simulations. For the TESSEL scheme, the variances and cumulative probabilities are best in agreement with observations when the unrouted data is smoothed over a time period that approached the TRIP simulations (see figure 7.12). In that case, however, the high frequency components are still under represented as was shown in figure 7.10.

Possible improvements

For applying the simple translation method, it was here assumed that the runoff was distributed equally over the river basins. Of course, this is a very rough assumption and there are multiple ways in which this translation method can be improved. For example, different weighting functions could be used to smooth the data to account for the unequal distribution of the runoff over the drainage area. An other way to improve this method is by applying it for each grid cell separately instead of considering the runoff from the

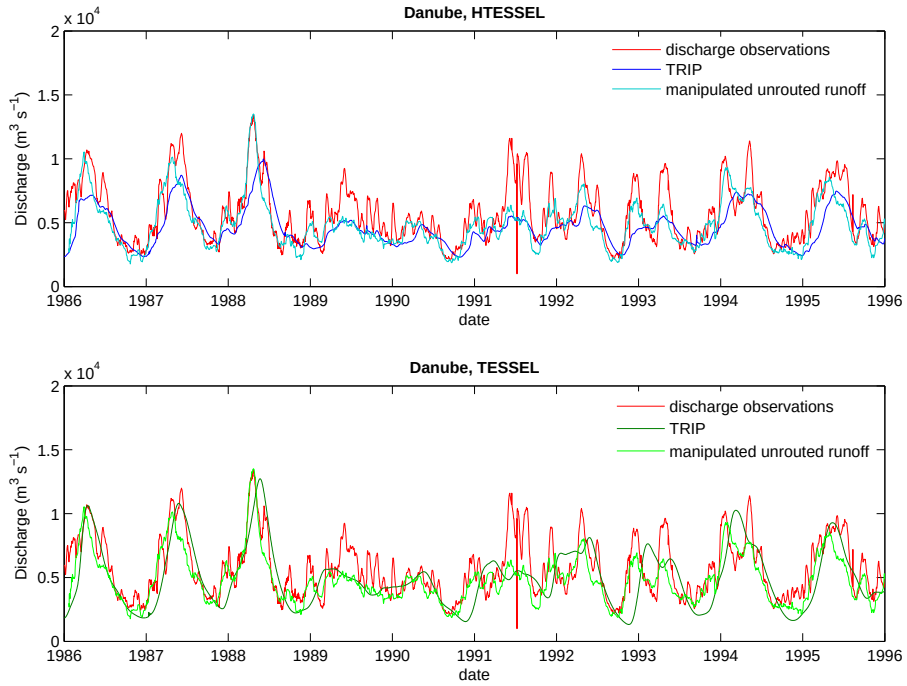

Figure 7.9: *Plots of the discharge observations, TRIP simulations and manipulated unrouted runoff for the* HTESSEL *(upper panel) and* TESSEL *(lower panel) scheme in the Danube. The unrouted discharge was shifted 20 days forward in time and smoothed over 40 days.*

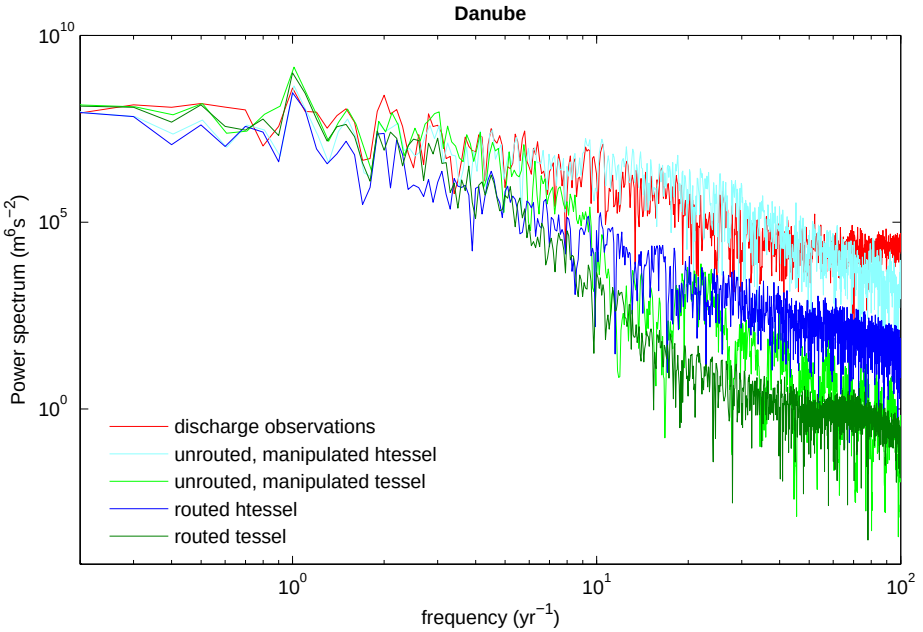

Figure 7.10: *Power spectrum of the routed and smoothed unrouted runoff simulations and of the GRDC-data. The figure shows that the high frequency components in the* TESSEL *runoff are underrepresented. The routed* HTESSEL *runoff also lacks high frequency components, but the spectrum of the smoothed unrouted* HTESSEL *runoff is better in agreement with the observations.*

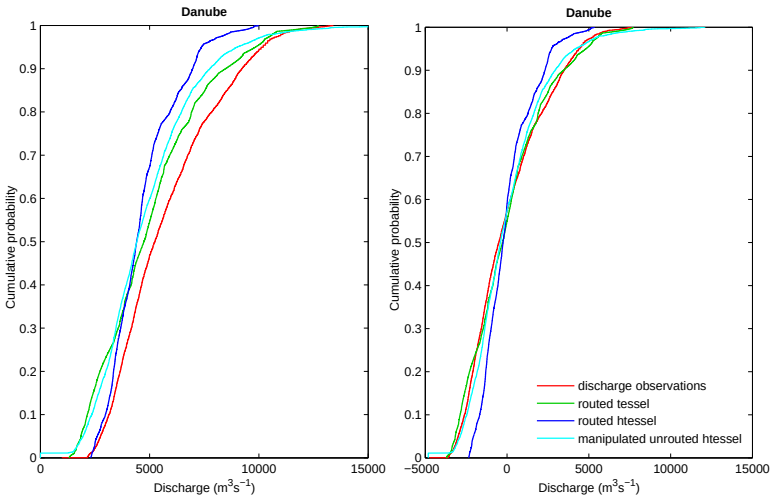

Figure 7.11: *Cumulative probability plots of the simulated and observed discharge in the Danube (at the river mouth) with (right panel) and without (left panel) subtraction of the 10-year average. The* HTESSEL-TRIP *simulation is plotted in dark blue, the* TESSEL-TRIP *simulation is plotted in dark green and the smoothed, unrouted* HTESSEL *and* TESSEL *runoff is plotted in light blue and light green respectively. Observations are plotted in red. There is an overall underestimation of the long term average which is about the same for both* LSMS*. The slope of the curve is best approached by the* TESSEL *simulations with delaying parameters n=0.01, τ_g=10 days. Good results are also found for the* HTESSEL *scheme by smoothing the* HTESSEL *runoff over 20 days.*

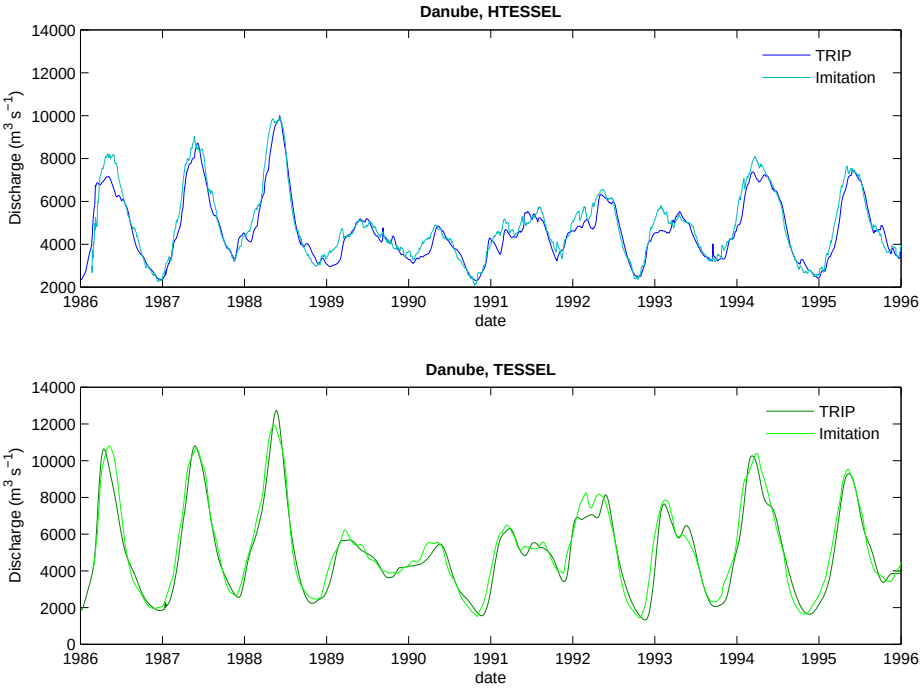

Figure 7.12: TRIP *simulations and imitations of the TRIP simulations for the Danube river for the* HTESSEL *(upper panel) and* TESSEL *(lower panel) schemes. To imitate the* TRIP *simulations for the Danube, the unrouted runoff is shifted 50 days further in time and smoothed by taking moving averages over 100 days.*

full drainage area. In this thesis, the simple manipulation method was only presented to show that a very simple approximation gives reasonably results (compared with the TRIP simulations). This indicates that the functioning of TRIP was not optimal or that the complicated river routing process in TRIP is unnecessary complicated for its purpose. Problems might for instance be caused when the parameterizations in the flow velocity algorithm do assume conditions that are not met in the streamflow through rivers or when the dimensions of the grid boxes in TRIP are too large to describe the slope of the river bed with the required accuracy.

7.7 Other rivers

A couple of other rivers were also considered for the validation. Figures 7.13 to 7.15 show observations, TRIP simulations and the manipulated unrouted runoff for different rivers. In most rivers, the high frequency variability was (in various extents) under-represented by the discharge simulations. This underestimation should probably partly be ascribed to the TRIP model, but in some regions the damped high frequencies should also be ascribed to the land surface models themselves (for instance in the Elbe region, see figure 7.16).

Furthermore, the runoff was heavily underestimated in the Mississippi river for both land surface models (see figure 7.17).

The quality of the discharge estimates by the simple translation method are in most regions at least comparable with the TRIP simulations. This might suggest that the TRIP scheme is unnecessary complicated for its purpose. It is also possible that the TRIP model did not function optimally. Although the delaying parameters in TRIP were tuned properly, some problems might have been caused by a too weak spin up criterion.

7.8 Conclusions

- For both LSMs, driven in the offline mode, the long-term averaged runoff is underestimated by almost 60% of the observed discharge in the Amazon and Mississippi region. Comparing the modeled runoff fractions in the Amazon (of about 0.2) with the observed runoff fraction (of 0.46) learns that the lack of runoff is probably explained by an overestimation of the evaporation by the LSMs.

- The observations of the Amazon discharge (at the river mouth) hardly contain variabilities with higher frequencies than once per year. Higher frequency variabilities in the runoff are filtered out by this large river. Since the TESSEL and HTESSEL scheme especially differ at small time scales (see section 2.4), the filtering of all high frequency variance by the river is not very convenient for the validation process. The remaining differences in the discharge is too small to pronounce judgment on which scheme behaves better.

- TRIP does not clearly improve statistical quantities such as the variance of the river discharge (compared with unrouted estimates of the discharge). For most performances, TRIP reduces the variance of the time series too strongly, resulting in an underestimation. Only when small delaying parameters are used, TRIP somewhat improves the variance of the TESSEL discharge simulations (compared with unrouted estimates). The variances of the HTESSEL simulations are deteriorated by all performances of the TRIP model (compared with raw, unrouted estimates of the discharge).

- When small delaying parameters are used in TRIP, the steepness of the cumulative probability curves improves (compared with unrouted estimates) for both models in the Amazone. In the Danube, an improvement of the cumulative probability curves

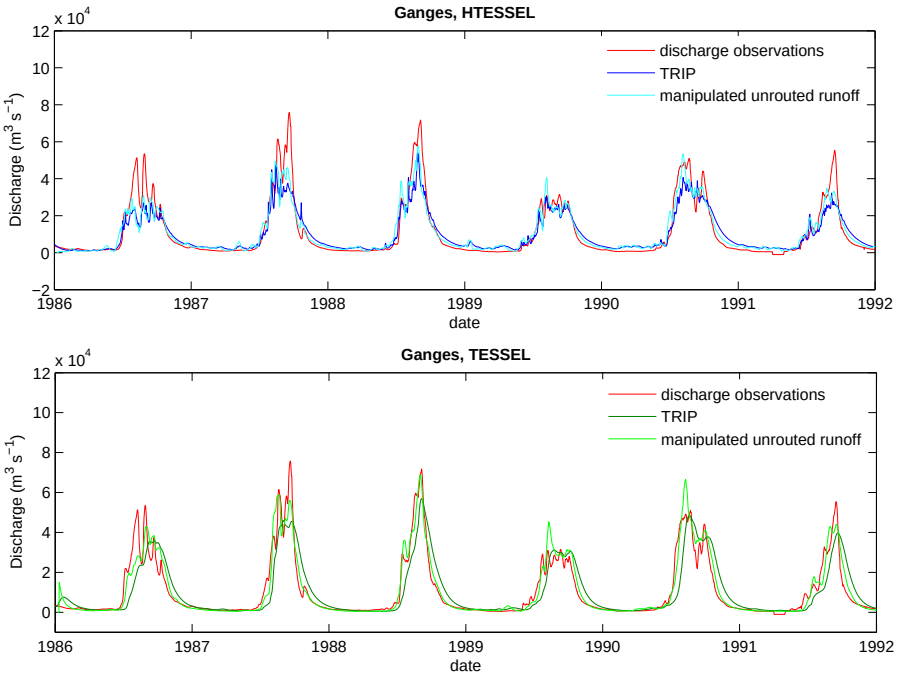

Figure 7.13: *Routed and manipulated unrouted* HTESSEL *(upper panel) and* TESSEL *(lower panel) runoff simulations for the Ganges river, shifted 5 days forward in time and smoothed by calculating moving averages over 10 days.*

of the TESSEL simulations can be obtained (for small delaying parameters), but the cumulative probabilities of the HTESSEL discharge estimates are deteriorated by all performances of the TRIP model.

- For the Danube river, the TESSEL-TRIP combination gives better estimates of the variance and the cumulative probabilities than the HTESSEL-TRIP combination. However, for both combinations the variance and especially the high frequency variance of the river discharge is underestimated.

- The high frequency variance of the unrouted TESSEL runoff is smaller than the high frequency variance in the observed discharge. For the TESSEL-TRIP combination, the underrepresentation of the high frequency components in the discharge is thus (partly) explained by an underrepresentation of high frequency variance in the raw, unrouted runoff and can thus (partly) be ascribed to the TESSEL land surface scheme.

- The unrouted HTESSEL runoff contains much high frequency variability. The underrepresentation of high frequency components in the HTESSEL-TRIP discharge simulations is probably due to too much smoothing by the TRIP scheme.

- The variance and cumulative probabilities of the HTESSEL river discharge in the Danube (as calculated by TRIP) can be improved by applying another translation method. This method translates the unrouted runoff simply by shifting the raw unrouted runoff in time and smoothing the time series over a certain time period.

- Also for other rivers, the river discharges could quite well be reproduced by this simple translation method. This might suggest that the TRIP scheme is unnecessary

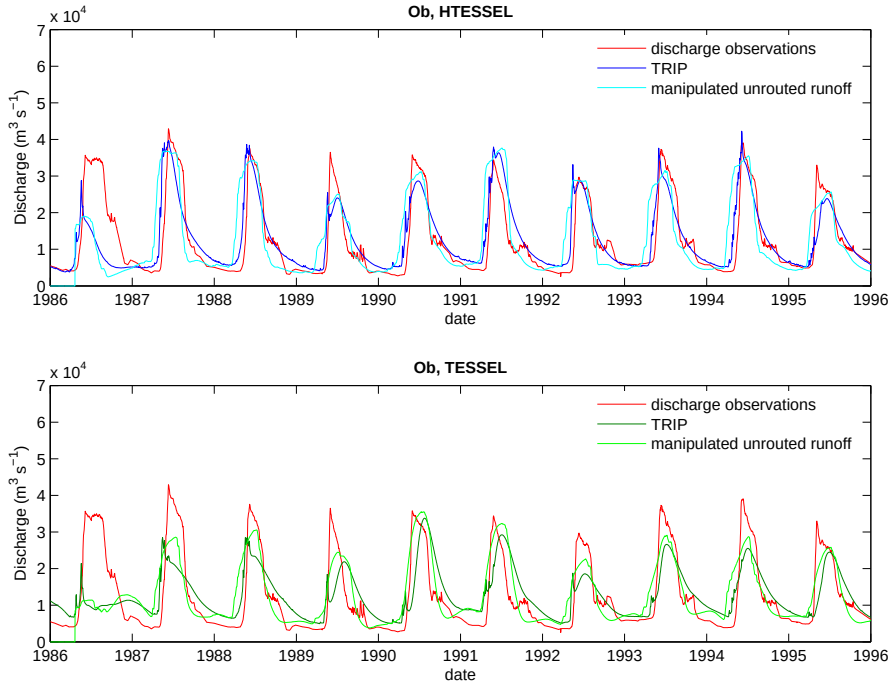

Figure 7.14: *Routed and manipulated unrouted unrouted* HTESSEL *and* TESSEL *runoff simulations for the Ob river, shifted 5 days forward in time and smoothed by calculating moving averages over 10 days.*

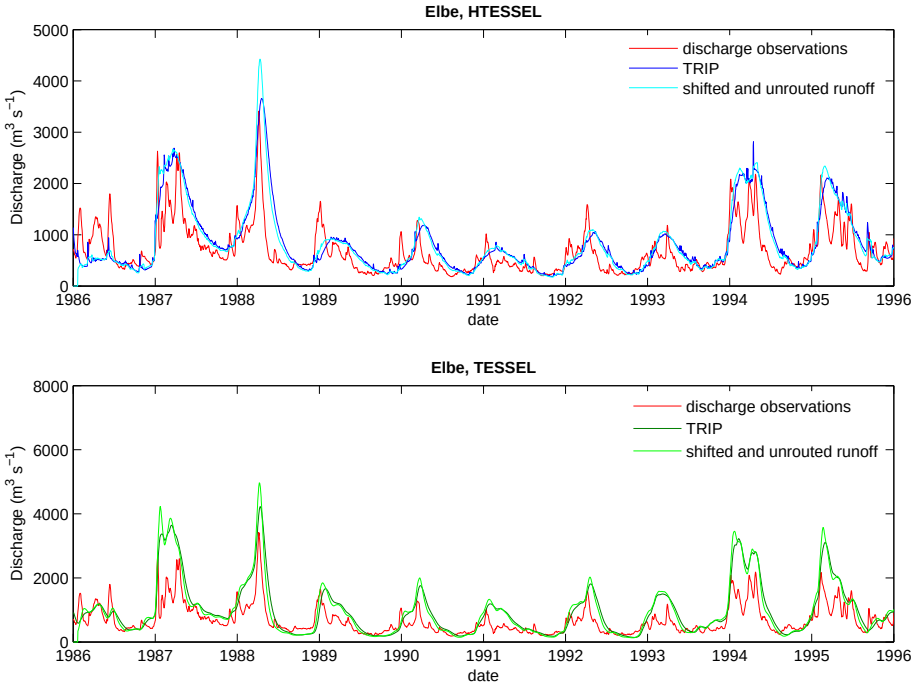

Figure 7.15: *Routed and manipulated unrouted* HTESSEL *and* TESSEL *runoff simulations for the Elbe river, shifted 5 days forward in time and smoothed by calculating moving averages over 10 days.*

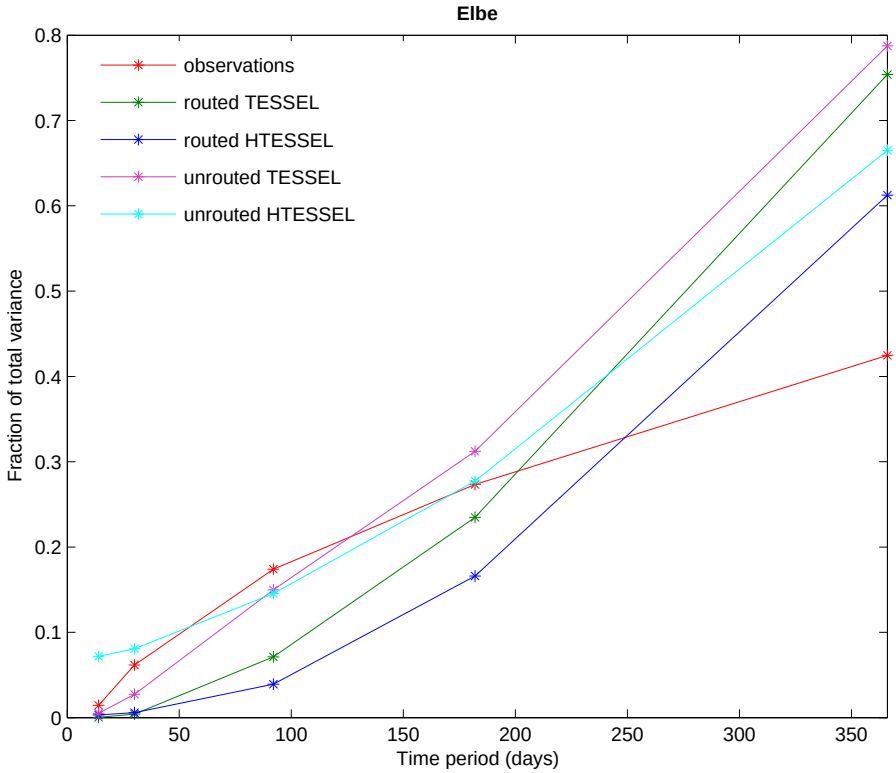

Figure 7.16: *The fraction of the total variance with specific time scales of up to two weeks, one month, three months, half a year and a year for unrouted* HTESSEL *(light blue), unrouted* TESSEL *(light green), routed* HTESSEL *(dark blue), routed* TESSEL *(dark green) and the* GRDC *discharge data (red) for the Elbe river. Considering the high frequency variabilities, the figure shows that the medium high frequency variability (with typical time scales of about 50 to 120 days) is underestimated by both land surface models. Also the low frequencies (of lower than once per year) are underestimated by both land surface models, whereas the contribution of frequencies between once per half year and once per year are overestimated.*

complicated for its purpose. Problems might for instance be caused when the parameterizations in the flow velocity algorithm do assume conditions that are not met in the streamflow through rivers or when the dimensions of the grid boxes in TRIP are too large to describe the slope of the river bed with the required accuracy. It might also be that the TRIP scheme did not function optimally.

- The variance of the TESSEL-TRIP discharge (which is also heavily underestimated) can not be improved in this way.

The most important results of this chapter are summarized in the diagrams of figure 7.18. This diagram compares the high frequency variability of the discharge observations, the TESSEL-TRIP and HTESSEL-TRIP discharge simulations and the (manipulated) unrouted runoff for the Danube. Variabilities with specific time scales of up to two weeks, up to one month, up to three months, up to half a year and up to one year were isolated by subtracting moving averages over the indicated time period from the original time series. The variances of the residues were determined and divided by the total variance of the original time series. The figure shows that high frequency variabilities are underrepresented in the unrouted TESSEL runoff, that TRIP damps the high frequency variability too much

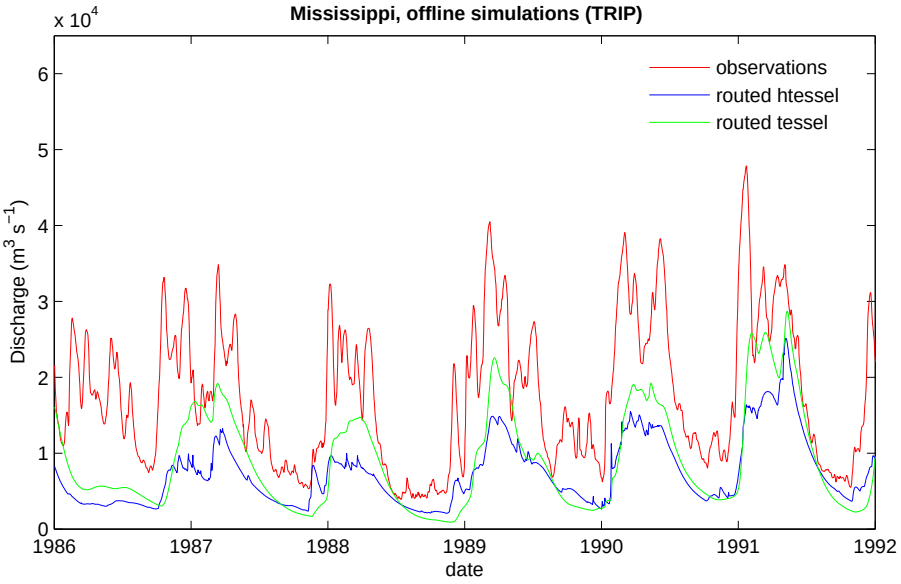

Figure 7.17: TESSEL-TRIP *and* HTESSEL-TRIP *discharge simulations for the Mississippi. The figure shows that both land surface models are underestimating the runoff with almost 60%. For both schemes the high frequency variability is under-represented (although the* HTESSEL *scheme gives slightly better results in term of high frequency variability than the* TESSEL *scheme).*

and that the high frequency variability can be represented reasonably well by a simple manipulation of the unrouted runoff.

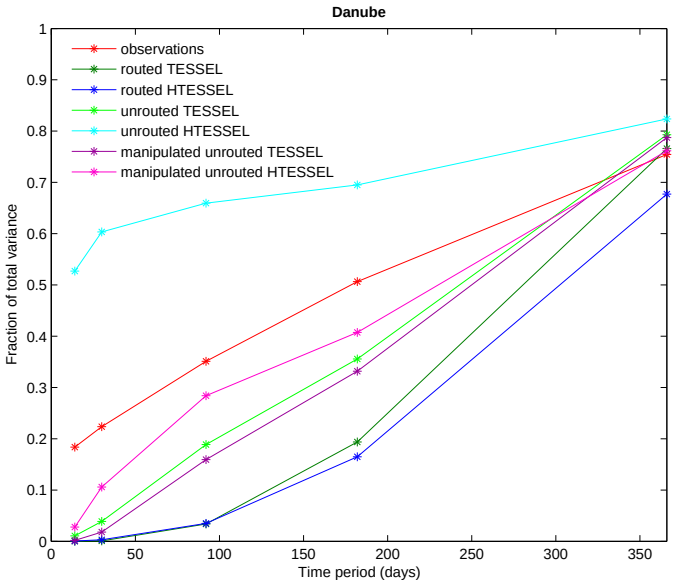

Figure 7.18: *The fraction of the total variance with specific time scales of up to two weeks, one month, three months, half a year and a year for unrouted* HTESSEL *(light blue), unrouted* TESSEL *(light green), routed* HTESSEL *(dark blue), routed* TESSEL *(dark green), the manipulated* HTESSEL *runoff (purple) and the* GRDC *data (red) for the Danube river.*

8

Online validation

For a complete validation it is necessarry to consider also the online functioning of land surface models (see section 2.3). Only by online validation, the induced feedback mechanisms for processes in the atmosphere can be assessed. In this chapter, climate simulations with the climate model EC-EARTH are considered.

The online validation of the land surface models, as it was performed in this project, is based on the comparison of the online modeled runoff with the offline modeled runoff (in which the land surface model was forced with atmospheric observations). It is assumed that when the climate is well modeled by the coupled system and the feedbacks between the climate model and land surface model are realistic, the surface water balances that are modeled with the coupled land surface model will approach the offline modeled water balances (since in that case the land surface model is driven by a similar atmosphere in both configurations). The questions addressed in this chapter are *How do the water balances as calculated by the climate model differ from the water balances as calculated by the offline land surface models?* and *Is the reliability of the climate simulations (of the runoff) limited by the atmospheric part or do the induced feedbacks mechanisms by the land surface models also play a role?* It was attempted to answer the second question by comparing the differences between the online and offline TESSEL runs with the differences between the online and offline HTESSEL runs. If the online simulations differ from the offline simulations for the TESSEL and HTESSEL model in a similar way, the atmospheric circumstances might especially be determined by the atmospheric model itself. If the deviations of the online from the offline simulations are different for both LSMS, the differences between the online and offline simulations should (partly) be ascribed to the effect of the LSMS on the atmosphere.

Modeled and observed precipitation fields and online and offline modeled runoff values were available. The online modeled precipitation was compared with observations and the online modeled runoff was compared with the offline modeled runoff. Since a climate model does not predict atmospheric conditions for one specific day, only statistical quantities (rather than the time series) were considered. Since the runoff was not directly compared with observations, raw unrouted runoff (rather than river discharges) has been used for the online validation.

8.1 Amazon

Figures 8.1 and 8.2 show maps of the seasonally averaged modeled and observed precipitation in the Amazon. The precipitation is underestimated by the climate model with about 40%. This leads to an underestimation of the runoff (figure 8.4). However, figure 8.4 shows that the online runoff is of comparable (rather than lower) magnitude as the offline runoff. This should be explained by different runoff fractions. The runoff fractions of the online simulations were found to be 0.38 (HTESSEL) and 0.35 (TESSEL) versus an observed runoff fraction of 0.46. These values are rather low, but do better agree with observations than the runoff fractions of the offline simulations (about 0.2 for both LSMS (section 7.1)).

Apparently, the reduction in the precipitation (of the online simulation compared with the offline simulation) does not lead to a reduction of the runoff (which is expected under identical atmospheric conditions), but to a reduction of the evaporation. The reduced evaporation indicates that the atmospheric conditions modeled by the climate model differ from the observed atmospheric conditions. The large underestimation of the precipitation and the small differences between the EC-EARTH-TESSEL and EC-EARTH-HTESSEL simulations (figures 8.3 and 8.4) indicate that the reliability of the climate simulations in the Amazon is probably limited by the atmospheric part of the climate model rather than by the land surface modules.

8.2 Danube

The precipitation is simulated rather well for the Danube region, although there is a considerable underestimation of the largest 60% of the precipitation (figure 8.5). The cumulative probability curve of the precipitation in the Danube (figure 8.5) is an example for what has also been found in other regions that were considered: the climate model has the tendency to underestimate the more extreme values of the precipitation.

Figure 8.6 shows that the 40% smallest values of the TESSEL evaporation are slightly smaller than the 40% smallest values of the HTESSEL values (irrespective of the configuration of the models), which is explained by the different behavior of the offline TESSEL and HTESSEL models. The largest 60% of the online simulated evaporation is smaller than the largest 60% of the offline simulated evaporation (irrespective of the LSMs), which is explained by the different atmospheric forcing on the online LSMs compared with the offline LSMs.

An other feature of the simulations in the Danube that was comparable with other regions is that the underestimation of the precipitation leads to a reduction of the evaporation (for the online compared with the offline simulations). Figure 8.6 shows that the online simulated runoff even exceeds the offline runoff, in spite of the underrepresentation of the modeled precipitation. This might suggest that (the statistics of) the atmospheric conditions in the climate model deviate from (the statistics of) the atmospheric observations. Figures 8.7 and 8.8 show that the runoff formation by the offline configured land surface models is more correlated with the precipitation, whereas the runoff formation by the coupled climate model is more correlated with the season (that is, to the atmospheric conditions). It is difficult to say whether this bias should be ascribed to the atmospheric part of the climate model (for instance by the underestimation of the precipitation) or that also the induced feedback mechanisms by the land surface models play a role. The small differences between the online TESSEL and HTESSEL simulations suggests that the deviating atmospheric conditions (of the simulations from the observations) should for a large part be ascribed to the atmospheric part of the climate model.

8.3 Conclusions

Conclusions of this chapter are:

- The precipitation in the Amazon is strongly underestimated by the climate model which results in a reduction of the modeled evaporation by the online models compared with the offline modeled evaporation. Both coupled models are not able to simulate the climate in the Amazon, which is probably explained by errors in the atmospheric part of the climate model rather than by the land surface models.

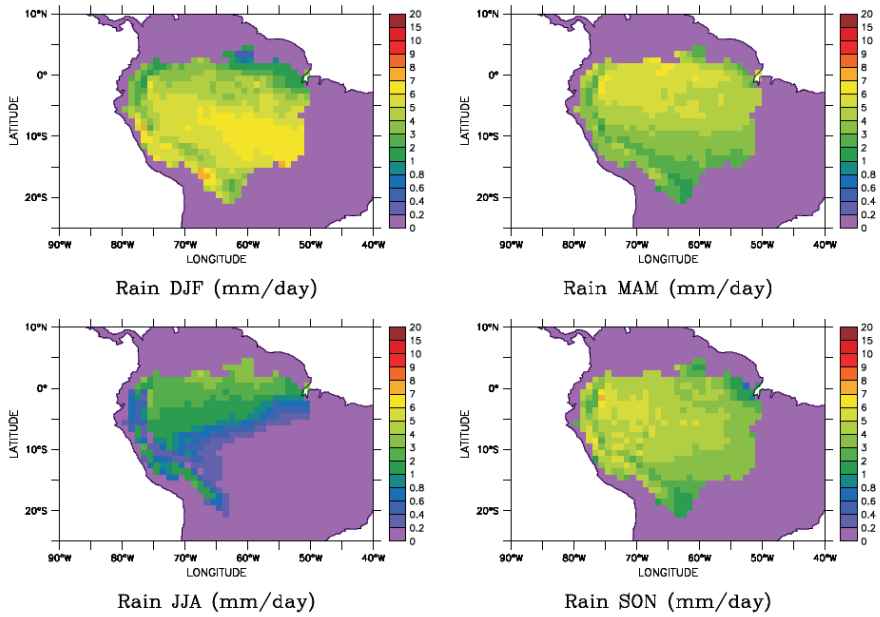

Figure 8.1: *Seasonal averages of climate simulations of the precipitationin in the Amazon region*

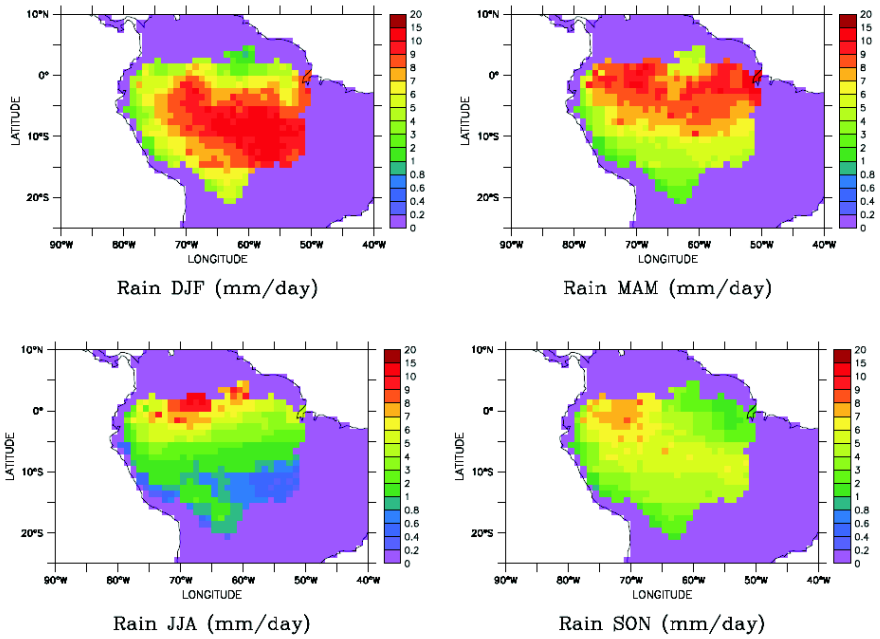

Figure 8.2: *Seasonal averages of the observed precipitation in the Amazon region, derived over the period 1986-1995*

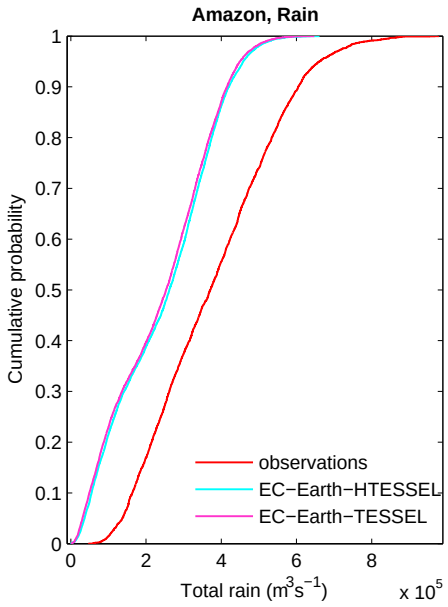

Figure 8.3: *Cumulative probability plots of the observed and modeled precipitation in the total drainage area of the Amazon (in m^3s^{-1}).*

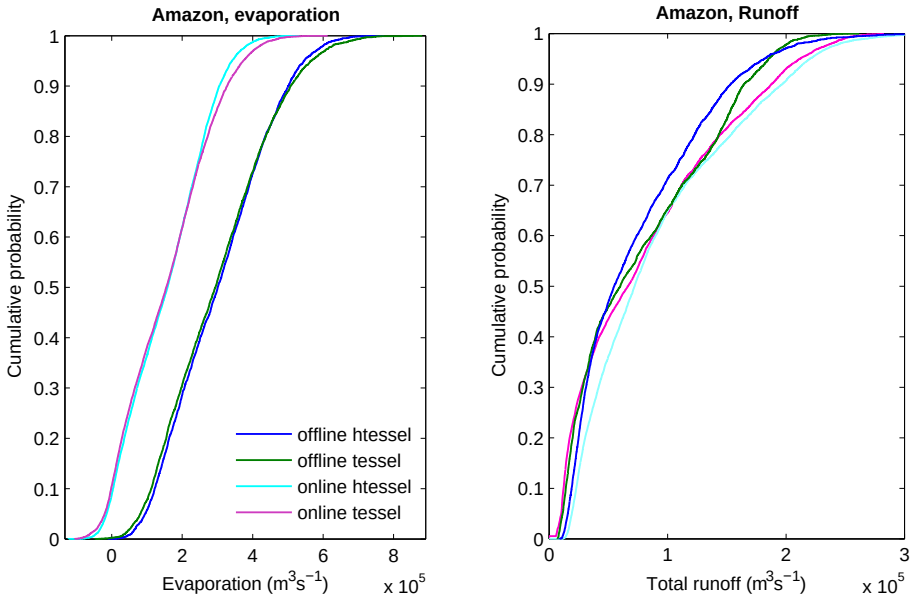

Figure 8.4: *Cumulative probability plots of offline and online* tessel *and* htessel *runoff simulations (unrouted) and of estimates of the evaporation (obtained from the difference between the precipitation and runoff simulations) for the Amazon .*

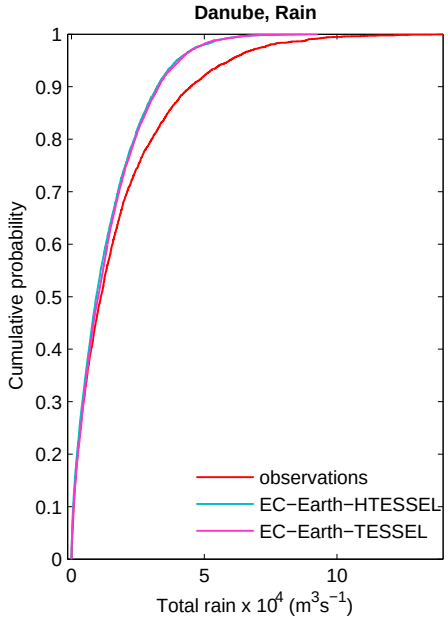

Figure 8.5: *Cumulative probability plots of the observed and modeled precipitation in the total drainage area of the Danube (in m^3s^{-1}).*

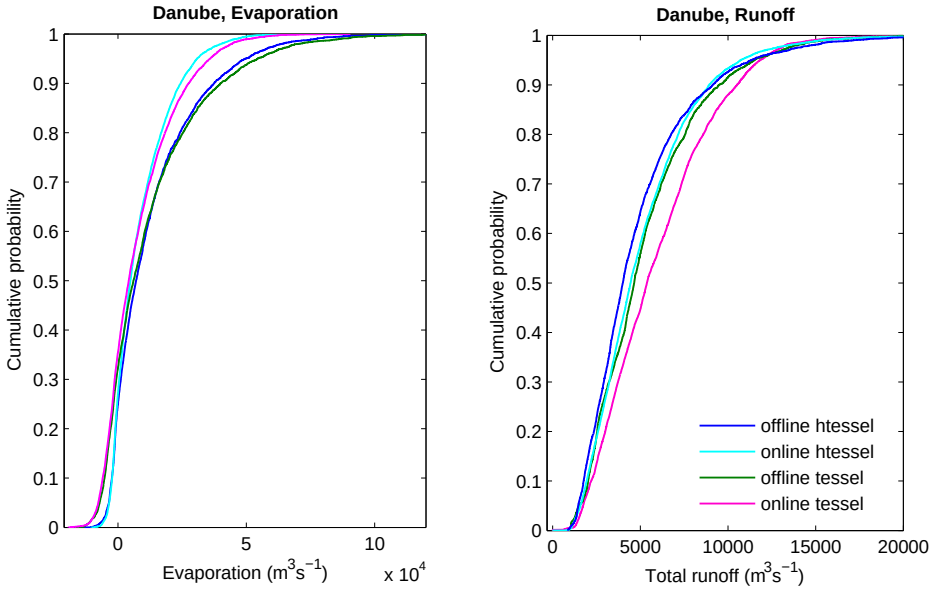

Figure 8.6: *Cumulative probability plots of offline and online* TESSEL *and* HTESSEL *runoff simulations (unrouted) and of estimates of the evaporation (obtained from the difference between the precipitation and runoff simulations) for the Danube .*

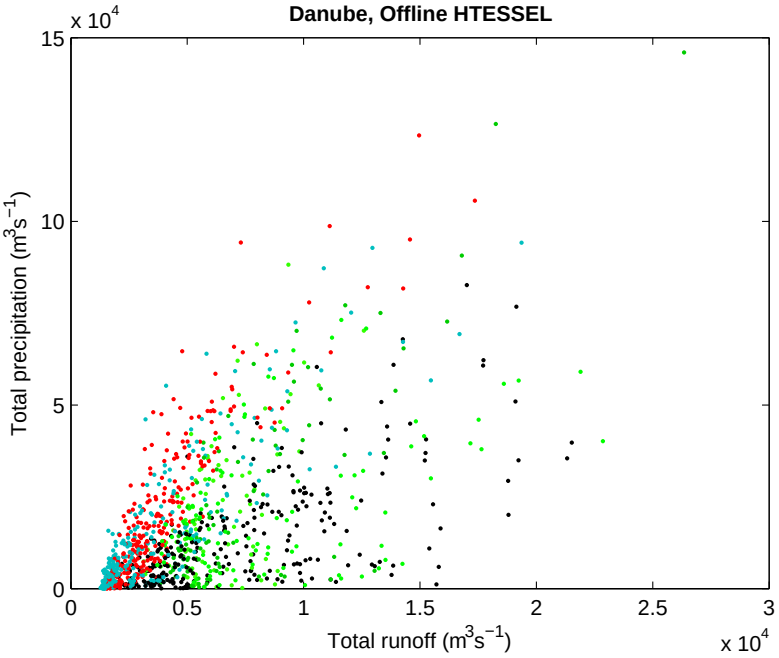

Figure 8.7: *The observed precipitation is plotted against the offline modeled runoff as to shows their correlation. The data-points indicate daily values of precipitation and runoff for the years 1986-1988. The different colors indicate different seasons: winter (black), spring (green), summer (red) and autumn (blue). The figure shows that, during all seasons, there is some correlation between the precipitation and the runoff.*

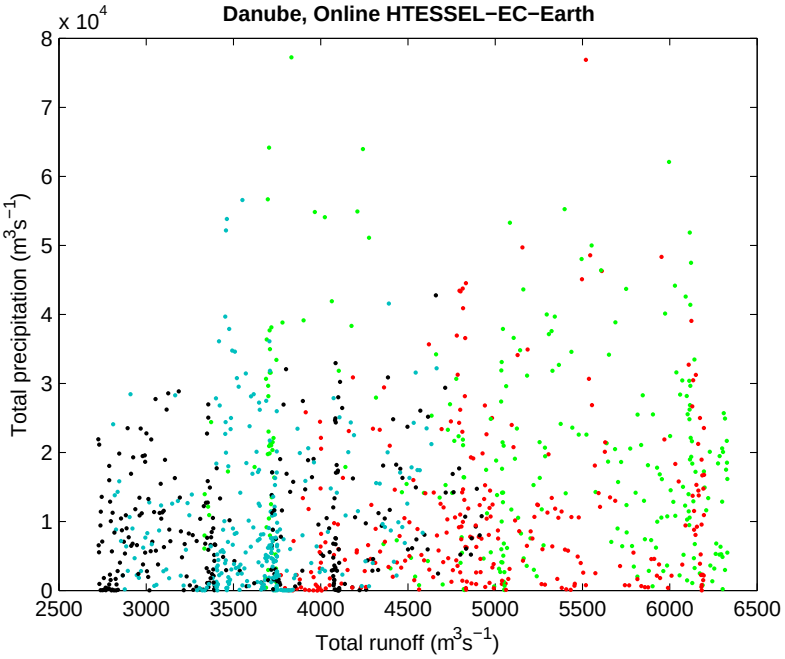

Figure 8.8: *The modeled precipitation is plotted against the online modeled runoff as to shows their correlation. The data-points indicate daily values of the first three years of the climate simulations. The different colors indicate different seasons: winter (black), spring (green), summer (red) and autumn (blue). The figure does not show a clear correlation between the runoff and the precipitation. Instead, in the climate simulations the amount of runoff seems to be more determined by the seasons.*

- The precipitation in the Danube is modeled fairly well, although there is a considerable underestimation of the largest 60% of the precipitation. This underestimation of the more extreme precipitations has also been found for other regions.
- The underestimated precipitation leads to a reduction in the evaporation (for the online compared with the offline simulations).
- the offline runoff formation is better correlated to the precipitation than the online modeled runoff. It is difficult to say whether this bias should be ascribed to the atmospheric part of the climate model (for instance by the underestimation of the precipitation) or that also the induced feedback mechanisms by the land surface models play a role.

9

Conclusions

The usefulness of the global river routing model TRIP for validating land surface models has been studied. First a sensitivity analysis was performed. It has been shown that the output variables of TRIP are influenced by parameters as the river slope and the river width. Compared with the other output variables, the discharge is less sensitive to uncertainties in these parameters and is most appropriate for testing land surface models and for making flood predictions. However, the parameters are influencing the time scale on which the outflow discharge adjusts to changes in the inflow and the velocity with which perturbations in the discharge are propagating towards the river mouth.

The effect of the TRIP scheme has been studied by comparing the routed and unrouted discharge. It has been shown that the most important function of TRIP is to delay and smooth the runoff. This results in a shift in the time series of the routed river discharge compared with the unrouted runoff. The delay of the water smoothes the time series of the discharge and reduces its variance and high frequency variability.

The TESSEL-TRIP and HTESSEL-TRIP discharge simulations were compared with observations. TRIP simulates the timing of the peaks in the discharge simulations reasonably well. However, the statistical quantities of the river discharge as the variance and the high frequency variance have a bias. The variance of the Amazon river discharge is underestimated, while the raw, unrouted runoff from the land surface models shows much variability. Also in the Danube, the variance and especially the high frequency variance is strongly underestimated, although the raw, unrouted HTESSEL runoff contains much high frequency variance. The use of the TRIP scheme for the validation of LSMs is especially limited by its tendency to delay the water too much and to damp the high frequency variability too strongly. This is unfortunate, since TRIP is purpose-designed to simulate river discharge and variations in the discharge at small time scales.

For comparison, an attempt was made to approach river discharges by shifting the spatially integrated unrouted runoff forward in time (a shift forward in time corresponds with a time delay) and smooth it by taking a moving average over a certain time period. This time period was optimized by considering the typical time lag of the discharge observations relative to the unrouted modeled runoff (however reasonable results were also found by considering the dimensions of the river basin and assuming a constant flow velocity between the 0.5 to 1 m/s). The method was applied for a couple of rivers. The quality of the obtained results are at least comparable with the TRIP simulations. This might suggest that the TRIP scheme is unnecessary complicated for its purpose. It might be worthwhile to reconsider the benefits of using a variable flow velocity algorithm. Does a variable flow velocity improve the discharge simulations or can comparable results be obtained by assuming a constant streamflow velocity? Maybe a better accuracy of parameters as the shape of the riverbed and the slope, defined on a more accurate grid (with a better spatial resolution), is required in order to make headway with the variable flow velocity algorithm.

Attempts were made to compare and validate the TESSEL and HTESSEL schemes, but

this was found to be quite difficult. Apparently, the Amazon river discharge is in essence not appropriate for the comparison and validation the land surface schemes. The high frequency variabilities in the runoff are fully filtered out by this large river. However, it is possible to validate some common features of both LSMs in the Amazon. By both LSMs, driven in the offline mode, the long-term averaged runoff in the Amazon is underestimated by almost 60% of the observed discharge. Comparing the modeled runoff fractions (about 0.2) with the observed runoff fraction (about 0.46) learns that the lack of runoff is explained by an overestimation of the evaporation by the LSMs.

For the Danube, the offline TESSEL-TRIP simulations were, in terms of variance and cumulative probability, better in agreement with observations than the offline HTESSEL-TRIP simulations. However, it has been shown that the high frequency components in the HTESSEL runoff were filtered out too much by the TRIP scheme. By shifting the spatially integrated unrouted runoff forward in time and smooth it by taking a moving average, it was possible to obtain realistic time series, variances, high frequency variabilities and cumulative probability curves of the river discharge in the Danube. The results obtained by this approach suggest that the short term variabilities in the river discharge are better simulated by the HTESSEL scheme.

Finally, an attempt has been made to compare the behavior of the TESSEL and HTESSEL land modules in an online model simulation, where the LSMs were coupled to the climate model EC-EARTH. The reliability of the runoff simulations by the coupled system is influenced a lot by the realism of atmospheric data (specifically the precipitation) which drive the LSMs. It was therefore difficult to determine the effect of the induced feedbacks on the atmosphere.

In most areas that were considered, the precipitation was (in various extents) underestimated by the climate model. A comparison between the online and offline modeled runoff indicates that in most areas the underestimation of the precipitation by the climate model leads to a reduction in the modeled evaporation (rather than to a reduction in the runoff). In the Danube region, the correlation between the runoff and the precipitation is under-represented by the climate model. These features might indicate that the modeled atmospheric conditions differ from observed atmospheric conditions. It is not clear whether this difference should be ascribed to the effect of the land surface model on the atmosphere or to errors in the atmospheric model itself.

Bibliography

[1] Balsamo, G., P. Viterbo, A. Beljaars, B. van den Hurk, M. Hirschi, A.K. Betts and K. Scipal; 2009. **A revised Hydrology for the ECMWF Model: Verification from Field Site to Terrestrial Water Storage and Impact in the Integrated Forecast System** -*J. Hydrometeor.*, **10**, 623-643.

[2] Chapelon, N., H. Douville, P. Kosuth, T. Oki; 2002. **Offline simulation of the Amazon water balance: a sensitivity study with implications for GSWP**-*Climate Dynamics*, **19**, 141-154.

[3] Decharme,B. and H.Douville; 2007. **Global validation of the ISBA sub-grid hydrology**-*Climate Dynamics*, **29**, 21-37.

[4] S.L. Dingman, K.P. Sharma; 1997.**Statistical development and validation of discharge equations for natural channels**-*Journal of Hydrology*, **199**, 13-35.

[5] Goosse,H., P.Y. Barriat, W. Lefebvre, M.F. Loutre and V. Zunz; 2009. **Introduction to climate dynamics and climate modeling**-*Online textbook available at http://www.climate.be/textbook*.

[6] Henderson-Sellers,A., K. McGuffie and A. Pitman; 1996. **The project for intercomparison of land-surface schemes:1992 to 1995**-*Climate Dynamics*, **12**, 849-859.

[7] Henderson-Sellers,A. and R.E. Dickinson; 1992. **Intercomparison of land surface parameterisations launched**-*EOS, Trans. Amer. Geophys. Union*, **73**, 195-196.

[8] van den Hurk,B., **Land Surface Schemes and Climate Models**. In: *Climate and the Hydrological Cycle*, M. Bierkens, H.Dolman,P.Troch (Eds.), IAHS, Oxford, 2008

[9] Leopold,L., W.G. Wolman and J.P. Miller; 1964. **Fluvial Processes in Geomorphology**, Dover, San Francisco. 522 pp

[10] Nijssen,B., D.P. Lettenmaier, X. Liang, S.W. Wetzel and E.F. Wood; 1997.**Streamflow simulation for continental-scale river basins**-*Water Resources*, **24**, 775-791.

[11] Pappenberger, F., G. Balsamo and H. Cloke; 2009. **Global routing with the hydrological component of the ECMWF NWP system**-*International Journal of Climatology*,accepted.

[12] Picher,P.L., V.K. Arora, D. Caya and R. Laprise; 2003.**Implementation of a Large-Scale Variable Velocity River Flow Routhing Algorithm in the Canadian Regional Climate Model (CRCM)** -*Atmosphere-Ocean* **41**, 139-153.

[13] Richards,K.; 1987. **Fluvial geomorphology**-*Progress in Physical Geography*, **11**, 432-457.

[14] T. Oki and Y.C. Sud; 1997. **Design of Total Runoff Integrating Pathways (TRIP)-A Global River Channel Network** -*Earth Interactions*. **2**, 1-37.

[15] The discharge data was obtained from *The Global Runoff Data Centre*, 56068 Koblenz, Germany.